Title: The comprehensive ontology of the anatomy and development of the solitary ascidian *Ciona*: the swimming larva and its metamorphosis.

Authors: Kohji Hotta[1]*, Delphine Dauga[2] & Lucia Manni[3]*

[1] Department of Biosciences and Informatics, Faculty of Science and Technology, Keio University, Kouhoku-ku, Yokohama 223-8522, Japan, khotta@bio.keio.ac.jp

[2] Bioself Communication, 28 rue de la bibliotheque, 13001 Marseille, France, contact@bioself-communication.com

[3] Department of Biology, University of Padova, Padova, Italy, lucia.manni@unipd.it

---

*Author for correspondence:

Kohji Hotta, Department of Biosciences and Informatics, Faculty of Science and Technology, Keio University, Kouhoku-ku, Yokohama 223-8522, Japan

E-mail: khotta@bio.keio.ac.jp

and

Lucia Manni, Department of Biology, University of Padova Via Ugo Bassi 58/B, 35121, Padova, Italy.

E-mail: lucia.manni@unipd.it

Running title: Ontology of anatomy and development of a solitary ascidian

---

29 pages of manuscript including references and figure legends

6 figures and 1 table

Additional files: 16

Abstract

Background: *Ciona robusta* (*Ciona intestinalis* type A), a model organism for biological studies, belongs to ascidians, the main class of tunicates, which are the closest relatives to vertebrates. In *Ciona*, a project on the ontology of both development and anatomy has been developing for several years. Its goal is to standardize a resource relating each anatomical structure to developmental stages. Today, the ontology is codified up to the hatching larva stage. Here, we present its extension throughout the swimming larva stages and the metamorphosis, up to the juvenile stages.

Results: To standardize the developmental ontology, we acquired different time-lapse movies, confocal microscope images, and histological serial section images for each developmental event from the hatching larva stage (17.5 h post-fertilization) to the juvenile stage (7 days post-fertilization). Combining these data, we defined 12 new distinct developmental stages (from Stage 26 to Stage 37), in addition to the previously defined 26 stages, referred to as embryonic development. The new stages were grouped into four Periods named: Adhesion, Tail Absorption, Body Axis Rotation, and Juvenile.

In building the anatomical ontology, 204 anatomical entities were identified, defined according to the literature, and annotated, taking advantage of the high resolution and complementary information obtained from confocal microscopy and histology. The ontology describes the anatomical entities in hierarchical levels, from the cell level (cell lineage) to the tissue/organ level. Comparing the number of entities during development, we found two rounds of entity increase: In addition to the one occurring after fertilization, a second one occurred during the Body Axis Rotation Period, when juvenile structures appear. On the other hand, a high number of anatomical entities (related to the larva life) are significantly reduced at the beginning of metamorphosis. Data were finally integrated within the web-based resource “TunicAnatO”, which includes several anatomical images and a dictionary with synonyms.

Conclusions: This ontology will allow for the standardization of data underpinning an accurate annotation of gene expression and the comprehension of the mechanisms of differentiation. It will help create an understanding of the emergence of elaborated structures during both embryogenesis and metamorphosis, shedding light on tissue degeneration and differentiation occurring at metamorphosis.

Keywords

Ascidian, anatomical ontology, metamorphosis, developmental stage, 3D, *Ciona*, morphology, database, confocal microscopy, histology

Background

Biological data including both spatial and temporal dimensions are essential for understanding the morphological organization of complex structures, such as tissues, organs, and organisms as a whole. Such structures, here called anatomical entities, once recognized and defined in a hierarchical way (*i.e.*, organized in an Anatomical Ontology, AO) and put in relationship with a developmental time-table specifying the developmental stage features (*i.e.*, a Developmental Ontology, DO), constitute the basis upon which to build an Anatomical and Developmental Ontology (ADO). The latter is a powerful instrument to standardize different kinds of biological data and an irreplaceable tool associated with model species [1–5].

Among tunicates, the sister group of vertebrates [6, 7], the solitary ascidians *Ciona robusta* and *Ciona intestinalis* (formerly *Ciona intestinalis* type A and type B, respectively [8–10]), are recognized model species for evolutionary, developmental, and ecological studies [11–14]. In the ascidian larva, the typical chordate body plan can easily be recognized and studied: Muscles for tail deflection during swimming flank a notochord; a hollow nerve cord is dorsal to the notochord, whereas an endodermal strand is ventral to it. This makes ascidians a privileged model for understanding the evolution of more complex vertebrates.

For *Ciona*, the anatomical and developmental ontology so far available regards 26 early developmental stages, from the unfertilized egg (Stage 0) to the hatching larva (Stage 26) [15]. This ontology is registered in the Bioportal web portal [16].

Moreover, representative 3D morphological reconstructions and optic cross-section images implement the ontology and are available in the web-based database FABA (https://www.bpni.bio.keio.ac.jp/chordate/faba/1.4/top.html). In FABA, information about cell lineages in early development was annotated based on previous investigations [17–20]. Considering that the ascidian embryogenesis is stereotyped, this ontology provides a standardized resource of spatial and temporal information for both *C. robusta* and *C. intestinalis*, as well as other solitary ascidians.

After larval hatching, ascidian larvae disperse, swimming freely and searching for a suitable substrate on which to metamorphose. The metamorphosis is deep and transforms the chordate-like larva into a sessile, filter-feeding adult (Additional file 1) [21]. In the latter, the chordate body plan is no longer recognizable, even if some other chordate features, such as the pharyngeal fissures (the stigmata) and the endostyle in the ventral pharynx (homologous to the vertebrate thyroid gland; Willey, 1893), are now visible.

To cover these further developmental phases, we decided to extend the ADO to the post-hatching larva development and metamorphosis. Here, we present this extension, which can be found in a web-based image resource, the FABA2 database (https://www.bpni.bio.keio.ac.jp/chordate/faba2/top.html), which follows the FABA approach and updates it. To build up this new part of the ontology, we conducted a deep anatomical investigation. The method of phalloidin-staining, successfully used for visualizing anatomical structures until the hatching larva stage [15], unfortunately was revealed as less useful, as cells shrink as development proceeds, thereby becoming hardly recognizable. Moreover, in differentiated individuals, low actin-based structures, such as the tunic or pigment cells (otolith and ocellus), are difficult to recognize. Consequently, we produced a comprehensive collection of both confocal scanning laser microscopy (CLSM) of whole-mount specimens, and light microscope images of 1-µm-thick histological serial sections of whole samples, for each developmental stage. For histology, specimens were cut according to the classical planes: transverse, sagittal, and frontal. This allowed us to build a complete anatomical atlas and was necessary for collecting the morphological information related to internal organs as well as the body shape and external surface. Lastly, for each anatomical entity, we annotated its definition, carefully checking the literature since 1893 and

considering, in particular, some milestones of ascidian literature, such as the exhaustive description of *C. intestinalis* published by Millar in 1953 [22]. Because the same anatomical structure was sometimes called different names by researchers in different Periods or belonging to different biological fields, we also annotated synonyms.

All this information, together with stereomicroscopy time-lapse movies, are consultable in the web-based resource called TunicAnatO (Tunicate Anatomical developmental Ontology) (http://www.bpni.bio.keio.ac.jp/tunicanato/top.html). TunicAnatO includes the former FABA database, therefore covering, in total, 37 developmental stages of *Ciona* development, from the unfertilized egg to the juvenile. TunicAnatO is also reachable via the Bioportal (http://bioportal.bioontology.org/), which is the most comprehensive repository of biomedical ontologies, and via the Tunicate Web Portal (http://www.tunicate-portal.org/), which is the main web tool for the Tunicate Community.

Results

The DO and AO from the Post-Hatching Larva Stage to the Juvenile Stage: working method

To construct the DO referring to the developmental stages of *C. robusta* following the hatching larva stage, time-lapse imaging and CLSM imaging of sequentially fixed specimens were performed (Fig. 1, Additional files 2-4). The DO presents the developmental stages grouped in Periods, which in turn are grouped into Meta-Periods, following the conventional nomenclature of ontologies (Table 1). Table 1 shows the 12 newly defined developmental stages, from Stage 26 to Stage 37. Moreover, it also introduces Stage 38 and Stage 39, here not described. These, together with Stage 40, complete the Juvenile Period of the Post-Metamorphosis Meta-Period (Additional file 4). The 12 new distinct stages correspond to six stages previously described by Chiba and collaborators [23]. With respect to our past tentative defining of the post-hatching stages, in the new database FABA2, we combined, in a single stage, the previous Stage 30 and Stage 31, because they are substantially similar. Representative images of individuals belonging to each stage, at both stereomicroscopy and CLSM, were chosen as a reference (Fig. 1; Additional file 3).

From now on, each entity, both developmental and anatomical, is written in bold when introduced for the first time; relations between entities appear in italics, while entity definitions appear between quotation marks. In the ontology, an identification (ID) code has been assigned to each anatomical and developmental entity. ID, which here is in brackets, is a set of numbers preceded by two prefixes. The first prefix is “Ciinte” when the ID was already introduced for *C. intestinalis* (used mainly for developmental stages, which are the same for *C. robusta*) and “Cirobu” when introduced for the first time in this ontology, which refers to *C. robusta*. The second prefix follows the first one and is “A” when the ID is referring to the anatomy and “D” when it is referring to development.

The larva stages considered here belong to the **Larva Period** (CirobuD:0000013), which is included in the **Embryonic Development, Pre-Metamorphosis Meta-Period** (CirobuD:0000003). The **Metamorphosis Meta-Period** (CirobuD:0000004) is divided into the following **Periods**: **Adhesion** (stage 30; CirobuD:0000013), **Tail Absorption** (stages 31-33; CirobuD:0000015), and **Body Axis Rotation** (stages 34-36; CirobuD:0000016). The **Post-Metamorphosis Meta-Period** (CirobuD:0000005) consists of the **Juvenile Period** (CirobuD:0000017). Overall, 39 stages (37 of which described and were integrated with original images) until the Juvenile Period was defined and combined with the previous ontology [15] (Additional file 4).

Once we defined the DO, we constructed the AO (Fig. 1). We carefully studied our anatomical data, comparing stage-by-stage information from CLSM and histology. This allowed us to recognize all the organs/tissues and follow their differentiation over time. We then listed, in an Excel file, the terms referring to the recognized anatomical entities (including synonyms, when present) used by researchers since 1893 (Additional file 5). We listed 206 entities (Additional file 6, column F, "Further specification 4"), assigning to each one its ID. Moreover, we detailed, for each anatomical entity, the following characteristics: the definition (column "Definition" in Additional file 6, Additional file 7) babondsed on the literature; the anatomical hierarchical level, specifying to which superior entity each belongs (*Part of*); the tissue from which it derives (*Develops from*); the developmental stage of its disappearance (*End stage*); and the developmental stage in which it is first recognizable (*Start stage*). Therefore, the *Start stage* and *End stage* relationships link the AO to the DO, furnishing the precise description of the timing of development. If necessary, we took note of a specific feature (column Comment in Additional file 6) and listed the bibliographic references (Additional file 5 and column Literature in Additional file 6). We also built a complete anatomical atlas in which most of the anatomical entities were efficiently annotated (Figs. 2-5; Additional files 8-14). Lastly, all the curated data were incorporated into a computable OBO format [24] (Fig. 1).

For example, for the entity **larval central nervous system** (CirobuA:0000579), the AO provides a consistent classification of cell types, tissues, and structures. Its relationship to the upper-level term **larval nervous system** (CirobuA:0000658) indicates that the larval central nervous system is *part of* the latter. The AO shows that the organ at stage 22 *develops from* its precursors, the A8.7, A8.8, A8.16, a8.17, a8.18, a8.19, a8.25, and b8.19 cell lines. In this example, the developmental relation is based on data from the cell lineage [18, 25, 26]. The larval central nervous system regresses (*End stage*) at stage 33 (Stage Late Tail Absorption) when most of the larval structures are reabsorbed at metamorphosis. The forebrain (*i.e.*, the anterior **sensory vesicle**, CirobuA:0000357), the midbrain (*i.e.*, the **neck**, CirobuA:0000657), and the hindbrain (*i.e.*, the **visceral ganglion**, CirobuA:0000778), are part of the **brain** (CirobuA:0000582). The forebrain contains 16 distinct entities, whereas the midbrain contains nine entities. The larval central nervous system includes four entities: **sensory vesicles** (CirobuA:0000938), **neck** (CirobuA:0000657), **visceral ganglion** (CirobuA:0000778), and **tail nerve cord** (CirobuA:0000740). Some of them include further sub-structures ("Further specification" columns in Additional file 6). For example, within the **sensory vesicle** (CirobuA:0000938), five further entities are included (anterior sensory vesicle, **posterior sensory vesicle** (CirobuA:0000696), **coronet cells** (CirobuA:0000890), **ocellus** (CirobuA:0000666), and **otolith** (CirobuA:0000671)), whereas the visceral ganglion includes the **motor neurons** (CirobuA:0000891). In addition, ependymal cells are included in the anterior sensory vesicles, neck, visceral ganglion, and tail nerve cord. For example, in the visceral ganglion, they are the lateral (CirobuA:0000643), ventral (CirobuA:0000776), and dorsal (CirobuA:0000606) visceral ganglion ependymal cells, respectively.

Below, we first describe how, where, and when the complex anatomical structures of *C. robusta* emerge and change during the Periods defined in this study. Then we present an overview of the number of anatomical entities and their appearance throughout the entirety of ontogenesis.

The Embryonic Development, Pre-Metamorphosis Meta-Period (Stages 26 to 29)

For the Embryonic Development, Pre-Metamorphosis Meta-Period, we described the last Period, called the Swimming Larva Period, during which the hatched larva (17.5hpf) swims actively, beating its tail. Although larvae belonging to this Period are generally defined as "swimming" larvae, their internal structures change significantly over time. Therefore, the Period (17.5-24 h after fertilization at 20°C) was divided into four anatomically distinguishable Stages, from Stage 26 to Stage 29, until the end of the locomotion phase.

Up to 90 entities are histologically recognizable as larval organs (Additional file 6). The main larval trunk territories are: the epidermis (CirobuA:0000619); the **endoderm** (CirobuA:0000615); the **mesenchyme** (CirobuA:0000653), mainly in the ventral-lateral trunk (**trunk ventral cells** (B7.5 line): CirobuA:0000748); and the nervous structures, such as the sensory vesicle, the ocellus, and the otolith, in the dorsal-mid trunk. The **nerve cord** (CirobuA:0000740), the **notochord** (CirobuA:0000665), the **muscles** (CirobuA:0000739), and the **endodermal strand** (CirobuA:0000616) are in the tail. As is typical in ascidians, the larva possesses three **adhesive papillae** (CirobuA:0000675) on the anterior trunk tip: two dorsal and one ventral.

The four Stages included in this Period exhibit the following features.

Stage 26

This is the **Hatching Larva Stage** (CirobuD:0000049; 17.5 h, Additional file 8). The larva has a roundish trunk and immature papillae (CirobuA:0000675) with round tips; it exhibits irregular **tail** (CirobuA:0000797) movements. Eight strips of **epidermal cells** (CirobuA:0000594) constitute the **tail epidermis** (Additional file 8A; CirobuA:0000738). The larval **pharynx** (CirobuA:0000682) shows a narrow lumen (Additional file 8B) [27]. The larval nervous system is subdivided into a central and peripheral nervous system. The former, as described above, contains several entities, for example, the otolith and the ocellus with **lens cells** (CirobuA:0000648), **photoreceptors** (CirobuA:0000683), and **pigment cup cells** (CirobuA:0000685); and the visceral ganglion with its motor neurons. The **larval peripheral nervous system** (CirobuA:0000681) is differentiating and each epidermal sensory neuron, *i.e.*, the **Rostral Tail Epidermal Neurons** (RTEN; CirobuA:0000709), the **Dorsal Caudal Epidermal Neurons** (DCEN; CirobuA:0000589), and the **Ventral Caudal Epidermal Neurons** (VCEN; CirobuA:0000757), shows dendritic arbors (Additional file 8A). A vacuolated notochord extends as an elongated structure in the tail (Additional file 8B). The **oral siphon primordium** (CirobuA:0000670) is in the form of an epidermal invagination not yet communicating with the pharynx lumen (Additional file 8). The **atrial siphon primordia** (CirobuA:0000368), the pair of invaginations of the dorsal-lateral trunk epidermis, called also **atrial placodes** (CirobuA:0000908), are not yet open to the exterior (Additional file 8D). The trunk is covered by a double-layered **tunic** (CirobuA:0000750) that, at this stage, is not well distinguishable at the histological level: the inner compartment of the tunic (CirobuA:0000882), bordered by the **inner cuticular layer** (CirobuA:0000883), and the **outer compartment of the tunic** (CirobuA:0000884), bordered by the **outer cuticular layer** (CirobuA:0000885) (see Additional file 9C^{I} for enlargement on the tunic).

Stage 27

This corresponds to the **Early Swimming Larva Stage** (CirobuD:0000050; 17.5-20 h; Fig. 2). The larva makes regular tail movements while swimming. The trunk elongates along the anterior-posterior axis. The **postpharyngeal tract** (CirobuA:0000871, Fig. 2C^{II}) is developing from the posterior pharynx and the **endodermal strand** [28] is histologically recognizable (Fig. 2C^{III}).

The **endostyle primordium** (CirobuA:0000617; Fig. 2C^{III}), *developing from* A7.1, A7.2, A7.5, B7.1, and B7.2 cells [27], is recognizable in the anterior pharynx. A wider lumen of the pharynx can be observed (compare Additional file 8C' and Fig. 2C', D). The atrial siphon primordia indent in the **posterior lateral trunk epidermis** (a7.14 and a7.15 cell lines) (CirobuA:0000916; compare Additional file 8C^{I} with Fig. 2D^{II}, E, and E^{II}). Mesenchyme cells in the posterior ventral trunk become round (Fig. 2D). Among sensory structures in the sensory vesicle (Fig. 2C and C^{II}), the **coronet cells** (CirobuA:0000890) can also be noted (Fig. 2B^{II}). These cells,

forming a hydropressure organ [29, 30], are considered by some authors to be the homolog of the vertebrate hypothalamus [31–33].

Stage 28

This is the **Mid-Swimming Larva Stage** (CirobuD:0000051; 20-22 h; Additional file 9). The papillae elongate and their basal part expands. The trunk is square in shape. The ciliary network belonging to the epidermal sensory neurons (**ascidian dendritic network in tunic**, ASNET; CirobuA:0000892) becomes more complex. The **preoral lobe** (CirobuA:0000901; Additional file 9C^{I}-C^{II}), a wide anterior body cavity between the pharynx and the anterior epidermis, is recognizable. Here, round mesenchyme cells are present. Spaces among the epithelia (**haemocele**, CirobuA:0000888) become larger; here, mesenchyme cells represent the **haemocyte** (CirobuA:0000571; synonym of blood cell) precursors. According to Parrinello and co-authors [34], haemocytes in adult animals are stem cells and granulocytes. The latter include clear granulocytes (precursors to clear vesicular granulocytes), microgranulocytes, and vacuolar granulocytes (including unilocular granulocytes and globular granulocytes). **Tunic cells** (CirobuA:0000751) are also recognizable in the inner compartment of the tunic (Additional file 9C-C'). They differentiate from mesenchyme cells. Coronet cells are well-differentiated on the left side of the sensory vesicle (Additional file 9C^{I}). The **otolith** (CirobuA:0000671) senses gravity at Stage 28 and gravitaxis is observed [35].

Stage 29

This is the **Late Swimming Larva Stage** (CirobuD:0000052; 22-24 h; Additional file 10). With respect to the previous stage, the trunk is longer and narrower, and the tail is longer. Moreover, the trunk profile is squared at the trunk-tail transition (Additional file 10A, C-C^{I}); in cross-section, the trunk and its tunic are polygonal and star-shaped, respectively (Additional file 10D-D^{VII}). All of the larval structures for swimming are fully mature: the **tunic fin** (CirobuA:0000622) located along the dorso-ventral axis, the **tail muscle** (CirobuA:0000739) fibers, and the tunic ciliated sensory fields (ASNET; Terakubo et al., 2010; Yokoyama et al., 2014). In *Ciona*, the larva swims by tail locomotion for several hours. The gravitaxis and visual behaviors are tightly interconnected at this stage [35]. The duration of the swimming period is variable among individuals. In our observations, it lasts until 23.6 hpf on average, *i.e.*, until the adhesion at the beginning of metamorphosis.

The **gut primordium** (synonym: "gut rudiment"; CirobuA:0000862) is histologically recognizable as endodermal tissue posterior to the pharynx. Here, the **protostigmata** (CirobuA:0000870) rudiments are now recognizable (Additional file 10B; [28]). According to Hirano and Nishida (2000), in *Halocynthia roretzi*, the atrial epithelium *develops from* A7.2, A7.1, A7.5, and B7.1 cell lines. It gives rise to the paired **atrial siphons** (CirobuA:0000366), not yet in communication with the **atrial cavities** (CirobuA:0000798) (Additional file 10C, D^{VI}).

Metamorphosis Meta-Period (24-60 h at 20°C, Stages 30 to 36)

In this Meta-Period, which is triggered by the larva adhesion, several anatomical changes are simultaneously observed, as the larval organs degenerate, whereas the adult organs appear and differentiate.

The Adhesion Period

The Adhesion Period (24-27 h post-fertilization at 20°C) consists of one stage: Stage 30 (Fig. 3).

Stage 30

The **Adhesion Stage** (CirobuD:0000053) regards the larva attaching to a suitable substrate through its adhesive papillae (24-27 h; Fig. 3). The mechanical stimulation of the papillae seems to be sufficient to induce tail regression ([36], submitted). The papillae change significantly after adhesion (Fig. 3A), becoming deflated and sometimes curved (Fig. 3A). They also start to degenerate. At this stage, the adhesion area is flat. Also called **holdfast** [27], in the successive stages it will elongate in the **stalk** (CirobuA:0000632), the epidermal peduncle by which the juvenile is attached to the substratum. The stalk possesses a cavity, derived from the preoral lobe (Fig. 3B^{II}), with its own **blood** (CirobuA:0000571) circulation.

The two atrial siphons are now in continuity with the atrial cavities. In the juvenile (Stage 40), the siphons will fuse, becoming a single, dorsal atrial siphon. The sensory organs are recognizable within the sensory vesicle but are beginning to degenerate (Fig. 3C^{III} and C^{vi}).

The inner and outer compartment of the tunic, with their inner and outer cuticular layer, respectively, are well recognizable (Additional file 9C^{I}).

The Tail Absorption Period

Immediately after the adhesion, the first observable change in the initiation of *C. robusta* metamorphosis, earlier than the onset of tail regression, is the backward movement of the posterior trunk epidermis ([36], submitted). The larval tail (**absorbed larval tail**: CirobuA:0000951) begins to be absorbed (27-30 h post-fertilization at 20°C). This Period consists of three stages: Stage 31, Stage 32, and Stage 33, whose duration depends on the extent of tail regression (Additional files 11-12). Although it is a short event of shrinkage, being completed within 75 min (Additional file 2) [37], it is very complex, simultaneously involving different tissues.

Stage 31

At the **Early Tail Absorption Stage** (CirobuD:0000054) 27-8 hpf; Additional file 11A-B^{I}), the shrinkage of the **tail epidermis** (CirobuA:0000738) begins at the tail tip (**Tail tip epidermis**: CirobuA:0000949) (compare Additional file 11B^{I} with Additional file 8B^{I}). In the same time, the tail epidermal cells, originally flat, change into thick and cuboidal (Additional file 11B^{I}). The actin staining in the posterior tail is relatively strong, indicating the actin's involvement in the shrinkage process [37]. In addition, the tail inner tissues, such as the notochord, the endodermal strand, and the muscles, begin to be arranged irregularly in the posterior tail region. In some individuals, the tail slightly bends at the trunk-tail transition (Fig. 1B, Stage 31). The otolith and ocellus are still present, although the larval brain is degenerating; their remnants will be recognizable during the Juvenile Period. The papillae, with their **dorsal palp neurons** (a8.18 line; CirobuA:0000601) and **ventral palp neurons** (a8.20 line; CirobuA:0000771), are no longer histologically recognizable at the end of the stage (*End stage*).

Stage 32

This corresponds to the **Mid Tail Absorption Stage** (CirobuD:0000055) 28-29 h; Additional file 11C-F^{III}), when 50% of the tail has been resorbed into the larval trunk. The tail is shorter and thicker than in the previous stage (Additional file 11C). The tail muscles contract together with the notochord; they fold and stack into the posterior trunk (Additional file 2, Additional file 11F^{I-II}). On the other hand, the **tail epidermis** (CirobuA:0000738) contracts without folding and finally invaginates into the trunk region. The process recalls the one described during the absorbing of the tail of *Halocynthia roretzi* and *Botryllus schlosseri* [38, 39]. Although the contribution of apoptosis is not excluded [40], it has been suggested that the tail epidermis and the extracellular **notochord sheath** (CirobuA:0000946) generate the strong forces retracting the axial organs into the trunk [39]. In fact, the tail absorption is inhibited by cytochalasin B, indicating that actin fibers play an important role in the process [41].

Concomitantly with tail absorption, the ASNET lose their organization [42].

The gut continues its differentiation. The **oral siphon** (CirobuA:0000668) opens. The **oesophagus** (CirobuA:0000621) [28, 43], the **stomach** (CirobuA:0000737) [23, 27, 28], and the **intestine** (CirobuA:0000635) [28] are histologically well recognizable. Also, the **heart** (CirobuA:0000628) is visible [44–48].

The **test cells** (CirobuA:0000915) are no longer present. They were originally encased in superficial depressions of the developing oocyte by the vitelline coat [23, 48–50]. After fertilization, they were moved into the perivitelline space, to attach to the outer cuticular layer of the tunic. At Stage 32, they are eliminated together with the outer tunic compartment layer and the outer cuticular layer (see Additional file 2). The stalk starts to elongate.

Stage 33

This corresponds to the **Late Tail Absorption Stage** (CirobuD:0000056; 29-30 h; Additional file 12), during which the tail becomes completely absorbed. Together with the tail, the 88 other larval entities associated with the embryonic and larval stages are no longer recognizable.

Both the notochord and the tail muscles are folded several times and coiled into the posterior trunk. Moreover, the posterior trunk epidermis wraps around the absorbing tail. Strong actin staining can still be observed in the absorbing axial organ (muscles and notochord) and in the degenerating tail epidermis.

In histological sections, several newly formed structures associated with the juvenile lifestyle can be defined. Some of them (annotated in Additional file 12) are the **body wal**l (CirobuA:0000857), the **atrial siphon muscles** (CirobuA:0000367), and the **pericardial cavity** (CirobuA:0000678) [43, 46, 47, 51]. The stalk continues to elongate. Tunic cells are numerous in the definitive tunic (the original inner compartment of the tunic with its inner cuticular layer).

The Body Axis Rotation Period

After the tail absorption, the **Body Axis Rotation Period** (CirobuD:0000016; 30-60 h post-fertilization at 20°C) occurs. Ascidian metamorphosis is characterized by the rotation of inner organs through an arc of about 90° (Cloney, 1982). The adult ascidian has a longitudinal body axis (the antero-posterior axis) that is parallel to the endostyle and passes through the oral siphon and the gut. In the adhering larva, the longitudinal body axis, easily individuated by the endostyle, is parallel to the substrate. During metamorphosis, it rotates progressively

so that, at the end of metamorphosis, it is almost perpendicular to the substrate and aligned with the stalk. This Period consists of three stages: Stages 34, 35, and 36 (Fig. 4; Additional file 13; Fig. 5), depending on changes in body shape (in particular, the enlargement of the branchial chamber due to protostigmata perforation) and the angle formed by the stalk axis (the definitive longitudinal body axes) and the endostyle axis. The latter, in early metamorphosis, does not correspond precisely with the oral siphon-gut axis, as the tail remnants occupy a large posterior body portion.

During this Period, many tunic cells in the tunic actively change their shape, forming filopodia, indicating that these cells are mobile and differentiated (Additional file 13A; Fig. 5A).

Stage 34

At the **Early Body Axis Rotation Stage** (CirobuD:0000057; 30-36 hpf; Fig. 4), the stalk continues to elongate and forms, with the endostyle axis, an angle of about 90°. The strong actin intensity in the trunk region close to the absorbed tail indicates that the latter is tightly packed (Fig. 4A^{I}, A^{IV}).

Adult organs proceed with their differentiation. In the digestive system (Fig. 4A^{II}, A^{IV}, B^{II}), the **pyloric caecum** (CirobuA:0000630) is differentiating evagination of the stomach. The latter starts to enlarge.

The **oral cavity** (CirobuA:0000802), representing the **oral siphon lumen**, extends to the rim of the **velum** (CirobuA:0000900) and **tentacles** (CirobuA:0000741, now recognizable (Fig. 4)[52–55]). The oral siphon lumen is in continuity with the **branchial chamber** (CirobuA:0000863; synonym: branchial sac, branchial cavity) lumen (Fig. 4A^{III}, B^{II}). Tunic cells are also in the tunic covering the inner oral siphon epidermis.

Stage 35

At the **Mid Body Axis Rotation Stage** (CirobuD:0000058; 6-45 h; Additional file 13), the endostyle axis is perpendicular to the axis passing through the stalk. In the branchial chamber, which is more expanded than in the previous stage, one pair of elliptical **gill-slits** (CirobuA:0000623), separated by a **transverse bar** (CirobuA:0000746), allows for filtration. The transverse bar contains the transverse sinus of the branchial sac. The **peripharyngeal band** (CirobuA:0000680), which is the ciliated band of the pharynx delimiting the **prebranchial zone** (CirobuA:0000869) from the branchial one, is visible [56].

Stage 36

At the **Late Body Axis Rotation Stage** (CirobuD:0000059) 45-60 h (2 dpf); Fig. 5), the angle between the endostyle axis and the axis passing through the stalk is 30°- 60°. With respect to the previous stage, some new entities are now recognizable. At the gut level, the **pyloric gland** (CirobuA:0000705) emerged from the pyloric caecum. At the neural system level, the **neural complex** (CirobuA:0000659), composed of the **cerebral ganglion** (CirobuA:0000582), and the **neural gland complex** (CirobuA:0000661) are distinguishable. The latter is formed of the **neural gland body**, which anteriorly exhibits a gland aperture, the **ciliated funnel** (CirobuA:0000584). The latter is located in the **dorsal tubercle** (CirobuA:0000932), on the roof of the prebranchial zone. Posteriorly, the neural gland body elongates into the **dorsal** strand (CirobuA:0000930). In the adult, a **dorsal strand plexus** (CirobuA:0000931) extends along the dorsal strand. Some **nerves** (CirobuA:0000929) are elongating from the neurons located in the cerebral ganglion.

The filter-feeding activity starts at this stage. Consequently, multiple entities linked to the respiratory and alimentary tract become physiologically functioning. Food, brought by water entering the oral siphon, reaches the branchial cavity (delimited by the **branchial epithelium** (CirobuA:0000677)) and passes through the oesophagus, the stomach, and the intestine (divided into the **proximal** (CirobuA:0000872), **mid** (CirobuA:0000655), and **distal intestine** (CirobuA:0000631)) for digestion. Fecal pellets are eliminated through the **anus** (CirobuA:0000362), which opens into the atrial chamber. In the branchial chamber, the endostyle is now characterized by its zones in the form of eight symmetrical longitudinal cellular bands (from the median **zone 1** (CirobuA:0000782) to peripheral **zone 8** (CirobuA:0000790))[27, 48]. It is involved in mucus production for filtration. The oral mechanoreceptor, the **coronal organ** (CirobuA:0000923), is developing on the oral tentacles and the velum. It controls the circulating seawater inside the animal body, together with the atrial **cupular organ** (CirobuA:0000924). The **circular muscular lumen** (CirobuA:0000859) and **longitudinal muscular system** (CirobuA:0000860), responsible for body contraction, become recognizable in the body wall. The heart, with its inner contractile **myocardium** (CirobuA:0000886) and outer **pericardium** (CirobuA:0000679) joined by a **rafe** (CirobuA:0000887), is now beating.

The Postmetamorphosis Meta-Period (3 days to over 7 days at 20°C, stages 37 to 43)

The **Postmetamorphosis Meta-Period** (CirobuD:0000005) consists of three Periods: the **Juvenile Period** (CirobuD:0000017), the **Young Adult Period** (CirobuD:0000018), and the **Mature Adult Period** (CirobuD:0000019). The Juvenile Period (3 days to over 7 days post-fertilization at 20°C) consists of five stages: 37, 38, 39, 40, and 41 (Additional files 4 and 14), defined mainly by gill slit and gut elaboration. Individuals still do not have mature reproductive organs, although gonads are developing. As reported above, this ontology includes only the description of Stage 37. The Young Adult Period consists of Stage 42 (2nd Ascidian Stage), corresponding to Stage 8 in Chiba et. al., 2004.

Stage 37

This is the **Early Juvenile I Stage** (CirobuD:0000060), which occurs when the endostyle axis is almost parallel to the axis passing through the stalk (63-72 h (3 dpf); Additional file 14). At this stage, the stomach swells and the larval tail remnants are no longer present (4 dpf).

The hermaphrodite **reproductive system** (CirobuA:0000909) is now recognizable. The **female reproductive system** (CirobuA:0000910) is formed by a sac-like **ovary** (CirobuA:0000672) continuous in an **oviduct** (CirobuA:0000801). The **male reproductive system** (CirobuA:0000910) comprises the lobular **testis** encrusting the ovary (CirobuA:0000742) and the **sperm duct** (CirobuA:0000920). **Germ cells** (CirobuA:0000916) are maturing within the gonads.

The stalk base forms **test villi** (CirobuA:0000927), each one furnished with a **test vessel** (CirobuA:0000928) in continuity with the haemocele. They ensure firm adhesion to the substrate. In the body, several **blood sinuses** (CirobuA:0000856) can be recognized among organs.

After Stage 37, other territories become histologically recognizable (data not shown). These are the **cloacal cavity** (CirobuA:0000852), the **dorsal languets** (CirobuA:0000636) on the roof of the branchial chamber (CirobuA:0000863), the **pharyngo-epicardial openings** (CirobuA:0000868) putting the **epicardiac cavities** (CirobuA:0000879) in communication with the branchial one, the **endostylar appendix** (CirobuA:0000866), the

oral pigment spots (CirobuA:0000899) and the **atrial pigment spots** (CirobuA:0000854) encircling the oral and the cloacal siphon border, respectively.

Number of anatomical entities and their appearance during ontogenesis

All the anatomical entities annotated in the ontology, from both actual results and previously reported data [15], were analyzed in whole during the complete ontogenesis of *C. robusta*. Figure 6 presents, stage by stage, their number from Stage 0 (unfertilized egg) to animal death. The graph shows that there are two rounds of tissue/organ increase. The first one is marked and occurs after fertilization; it reaches a plateau at about Stage 12 (Mid-gastrula), when about 121 entities are recognizable. At Stage 34 (corresponding to the conclusion of the Body Axis Rotation Period), there is a sharp decrease in the number of entities, which suddenly drops to about 90. This decrease is followed by a slight second increase that reaches a plateau (of about 112 entities) in the Juvenile Period.

The *Start stage* and *End stage* relations also furnish a view of how long an entity is present along ontogenesis (Additional file 15). Ninety-three entities are specific to the larva: They develop during embryogenesis for the active larval life but are resorbed during metamorphosis. Twenty entities (such as the epidermis, inner compartment of the tunic, and tunic cells) are recognizable throughout ontogenesis: They appear during embryogenesis but are not eliminated at metamorphosis. They are persistently present during the larval life, metamorphosis, and juvenile/adult life. Lastly, 91 entities characterize the juvenile/adult life, as they form during metamorphosis, differentiate during the Juvenile Period, and continue to grow during adult life, following the increase in size of the animals [22].

Discussion

The ontology of *Ciona robusta*: a powerful tool for developmental biology studies

C. robusta is considered a valuable model for studying the developmental biology of tunicates and the evolution of chordates. For this species, several databases have contributed as resources for genome and gene expression information (*e.g.*, Ghost, http://ghost.zool.kyoto-u.ac.jp/indexr1.html; CITRES, https://marinebio.nbrp.jp/ciona/) and proteomic studies (e.g., CIPRO, http://cipro.ibio.jp/), or furnish technical information (*e.g.*, ACBD, the Ascidians Chemical Biological Database, https://www.bpni.bio.keio.ac.jp/chordate/acbd/top.html). All the available databases are easily consultable via the Tunicate Web Portal (https://tunicate-portal.org/). In this study, we present the database TunicAnatO, which implements the previous database FABA [15] and is devoted to anatomy and development. Moreover, the ADO built here is combined with the ANISEED database (https://www.aniseed.cnrs.fr), which provides high-throughput data and *in situ* experiment data from the literature for ascidian species. Therefore, we integrate the panorama of actual databases and offer a tool that will help researchers recognize the anatomical structures of their interests. This will allow for the standardization of data underpinning an accurate annotation of gene expression and the comprehension of mechanisms of differentiation.

The developmental ontology

In this work, merging the previously reported developmental stages [15, 23], with new data from stereomicroscopy, CLSM, and histology, we implemented the description of the whole life cycle of *C. robusta*, from fertilization to juvenile. The whole development has been divided into Meta-Periods, Periods, and Stages,

following the canonical temporal subdivision of developmental ontologies [23]. Using a low-resolution stereomicroscope to examine larvae, metamorphosing individuals, and juveniles for dissection, we defined the new subdivision into stages. The simplicity of stage recognition is a prerequisite for a good staging method. Researchers will easily be able to discriminate stages, using a simple instrument, a stereomicroscope, when checking the development of their living samples in the laboratory after *in vitro* fertilization, or when analyzing fixed whole-mount specimens.

We introduced 12 new stages (from Stage 26, Hatching Larva, to Stage 37, Early Juvenile I) that add to those already reported up to the Larva Stage [15]. Therefore, 37 stages are now described in detail and documented with original images. Considering that we also defined (without describing) Stage 38 (Early Juvenile II) and Stage 39 (Mid Juvenile I), once they are described, the whole Juvenile Period will be completed. The lacking steps are, then, the Young Adult Period (Stage 40) and the Mature Adult Period (Stage 41). However, for the latter Period, the exhaustive anatomical description by Millar [22] is still an essential reference. In summary, the whole life cycle of *C. robusta* is almost described and annotated. This is an important result, considering that ontologies regarding other model organisms are limited to embryogenesis [1–5].

It should be noted that, in annotating the progressive organ appearance and degeneration, we could also describe in detail the metamorphosis process, whose general reports for ascidians are dated, not so accurate and timed, and limited to a few species (see for review: [20, 48]). Only some specific processes occurring during metamorphoses, such as tail regression [37, 57] or papillae retraction [57], have been described in detail in *C. robusta*.

The anatomical ontology

This study underlines the importance of a combined analysis of data. In fact, for each stage, we examined corresponding high-resolution images thanks to CLSM and histology. The two methods have advantages and disadvantages in terms of studying anatomy. CLSM furnishes high tissue resolution and relatively rapid processing, so it allows for the analysis of multiple samples. Moreover, in automatically making z-stacks, we can quickly obtain 3D reconstructions. However, tissues/organs can be difficult to recognize due to the limited number of fluorochromes that can be simultaneously used. Moreover, a low laser penetration can be a limit for the study of thick specimens. On the other hand, histology offers (other than a high tissue resolution) ease in tissue/organ recognition thanks to the different tissue affinities to labeling. However, the method is time-consuming, which means that few samples can be analyzed, and 3D reconstructions are not automatically generated. Therefore, we used, in combination, the complementary information coming from these two working methods, making it possible to identify, with precision, the inner structures as well as the outer surface of individuals, annotating in total 204 anatomical territories.

To build the hierarchical tree of anatomical entities (specified by the relation *Part of* in Additional file 6) and to define each of them (complete with synonyms), we consulted several publications covering over 120 years of literature on *Ciona* and other ascidians, from 1893 [58] to today. Fundamental references for creating the dictionary were, among others, those published by Millar [22], Kott [59], Burighel and Cloney [48], Chiba and collaborators [23], and the last description of the species by Brunetti and collaborators [8]. We also consulted the glossary TaxaGloss (https://stricollections.org/portal/index.php).

The AO is documented by the database TunicAnatO, which is an anatomical atlas of original images readily available via the internet and easily accessible from any standard web browser (http://www.bpni.bio.keio.ac.jp/tunicanato/top.html). This database contains information from both z-slice sections and 3D reconstruction images, and histological sections at each time point along the developmental course of *C. robusta*. In images, the anatomical entities were labeled, furnishing a guide for tissue recognition.

Data integration in anatomical and developmental ontology

In this work, we linked DO and AO in a comprehensive DAO, as we defined, for each entity, the relations *Develops from*, *Start stage*, and *End stage*. These relations were determined at the cell level when cell lineage data were available and at the tissue/organ level where complexity did not allow for the following of cell genealogy. Lastly, when possible, we also annotated features linked to organ functionality (swimming, feeding, respiration, or heart beating). Some entities showed multiple possibilities to be defined, while others had uncertain/controversial definitions.

In some cases, and where possible, we defined the anatomical entities according to multiple organizational levels. For example, the "atrial siphon muscle" *Start stage* is Stage 10 if we refer to cell lineage [43, 46, 47, 51], while it is Stage 33 if we refer to histology (muscles recognizable on sections) and Stage 36 if we refer to the functional state of the muscles (ability to contract). Similarly, the *Start stage* for the "endostyle" is Stage 27 if we refer to the cell lineage [27], while it is Stage 34 if we consider the presence of its main histological features (its subdivision into eight symmetrical zones, visible on sections) and Stage 36 if we refer to its physiological activity during feeding (mucus production trapping food particles). It should be noted that, because for *C. robust*a there is no cell lineage of the endostyle, we referred to data from *Halocynthia roretzi* [27]. These and other, similar examples, exhibiting multiple tissue recognition levels, are all annotated in the ontology (among the Comments in Additional file 6), for a comprehensive view of development.

In other cases, we found entities critical to define, as publications do not fully agree with each other. One case was that of the "neural crest-like cells", a cell population very important from an evo-devo perspective because it is considered a homologue to the vertebrate neural crests [51]. Indeed, the *Start stage* is Stage 10 according to Stolfi and collaborators [60] and Jeffery and collaborators [61], but it is Stage 13 according to Abitua and collaborators [62].

Also, the relation *End stage* presented some critical aspects. For example, always considering the neural crest-like cells, the *End stage* depends on their derivatives and the species. According to Jeffery and collaborators [61], in *Ecteinascidia turbinata*, the neural crest-like cells form the adult pigmented cells; therefore, the *End stage* is animal death. However, in *Halocynthia roretzi*, two undefined cell pairs (b7.13 derived) were reported in the posterior-dorsal region of the tail [63]. In this case, therefore, the *End stage* corresponds to the tail absorption at metamorphosis (Stage 33). In *Ciona* [64], the same cells also seem to be present under the dorsal epidermal cell layer; the *End stage* in this case in not determinable, as the destiny of these cells is unknown. Also, this and other, similar critical situations are reported in the section "Comments" of the ontology.

All the above-reported examples highlight the complexity and choices underlying the ontology building. However, the presence of comments associated with each entity in this ontology, and the huge number of citations reported, assure users of a comprehensive view of *C. robusta* anatomy and development.

An analysis of other ontologies currently available shows that the ontology of *C. robusta* presented here is very rich in information. Sixty-one ontologies deal with anatomy on FAIR sharing (https://tinyurl.com/ybhhfd8c) [65]. Among them, 12 describe the anatomy of animal model organisms (*e.g.*, *Drosophila*, *Caenorabditis elengans*, mosquito, mouse, zebrafish, *Xenopus*, planaria, the ascidian *Botryllus schlosseri*). In terms of a comparison of the ontology of *C. robusta* presented here with the latter (Additional file 16), the first one possesses very rich lineage information compared to other ones. Moreover, among the 12 above-mentioned ontologies, four combine developmental stages and anatomical terms, eight include the relation *Develops from*, and 10 use references as a source of data. The ontology of *C. robusta* exhibits all these features. It is to be considered, however, that ontologies are never-ending tools. They must be continuously updated when new information becomes available.

An overview of the ontogenesis of *C. robusta*

Thanks to the annotation of the relations, *Start stage* and *End stage*, we could verify, in *C. robusta*, the progressive emergence—and, where appropriate, disappearance—of its unique features. Looking at them as a whole, we obtained a global view of ontogenesis.

Our results show that ascidians have two rounds of increasing complexity: the first one during cleavage until gastrulation, and the second one during metamorphosis. This can reflect the development of structures associated with the larval life (104 in total; for example, the larval nervous system, the tail with associated notochord and muscles) and with the juvenile/adult life (80 in total; for example, the branchial basket, the gonad, the gut). Other structures (20 in total) are, of course, persistent throughout the whole ontology: They are, for example, the epidermis, the tunic, and the hemocytes.

Moreover, we show that almost half of the anatomical structures disappear during metamorphosis. This occurs during the Tail Absorption Period, when structures exclusively formed for the larval life degenerate. This drastic event was not previously documented quantitatively. It should also occur in other invertebrate species, such as barnacles and sea urchins [66, 67]. Also in barnacles and sea urchins, in fact, there is the loss of many organs associated with the motile larva that metamorphoses in a stationary form. Such a sharp decrease in anatomical structures was not reported in other chordate animals. It would be interesting to verify if a sharp decrease in anatomical structures occurs also in ammocoetes and frogs, which undergo a drastic metamorphosis comparable to that of tunicates..

Conclusions

In this study, we present the anatomical and developmental ontology of the ascidian *C. robusta*, from the swimming larva stage, through metamorphosis and until the juvenile stages. We newly define 12 stages that, together with the previously described stages related to embryogenesis, extend our knowledge to almost the whole ontogenesis. This ontology, furnishing the hierarchical description of more than 200 anatomical entities, complete with definitions, synonyms, and bibliographic references, provides the guideline for several functional studies on tunicate cell biology, development, and evolution. It allows for the standardization of data underpinning the accurate annotation of gene expression and the comprehension of mechanisms of differentiation. It will help in understanding the emergence of elaborated structures during both embryogenesis and metamorphosis, shedding light on tissue degeneration and differentiation occurring at metamorphosis.

Methods

Biological materials, preparation of embryos for time-lapse imaging

C. robusta adults, provided by NBRP, were obtained from the Kyoto bay and Tokyo bay areas in Japan. Eggs and sperm were obtained surgically from gonoducts. After insemination, eggs were maintained in agarose-coated dishes with Millipore-filtered seawater (MFSW) containing 50 µg/ml streptomycin sulfate, and the early cleavages were uniformly synchronized (data not shown). To keep the temperature stable, we used a Peltier-type incubator (CN-25B, Mitsubishi, Japan) without any vibration to prevent embryo fusion. Embryos developed in hatched larvae approximately 18 h after insemination.

The hatched larvae were maintained in plastic dishes on the thermo-plate at 20°C to acquire images. Using a digital camera (Olympus SP-350) mounted on a microscope, images were acquired every 3 to 10 min for 7 days (Additional file 2). After 3 days post-fertilization, food was given (vegetal plankton, sun culture).

Although the timing of metamorphosis showed a huge deviation depending on the timing of adhesion, we considered an average timing, looking at animals exhibiting a representative morphology.

Image acquisition at confocal scanning laser microscopy (CLSM)

Fixed specimens were prepared at different timings of development, from hatching larva up to 7dpf juvenile. Samples were fixed for 30 min – 1 day at room temperature in 4% EM grade paraformaldehyde (nacalai tesque code 00380) in MOPS buffer (0.1 M 3-(N-Morpholino) propanesulfonic acid), adjusted to pH 7.5. Specimens were then washed three times with phosphate-buffered saline (PBS) and incubated in Alexa-546 phalloidin (Molecular Probes, Eugene, OR) in PBS containing 0.01% Triton X-100 (PBST) either overnight at 4°C or at room temperature for 1-2 h. Specimens were then rinsed for 3 min in PBS, attached to glass slide dishes, dehydrated through an isopropanol series, and finally cleared using Murray clear, a 2:1 mixture of benzyl benzoate and benzyl alcohol. Alexa 546 phalloidin was used to visualize cell membranes because it stains mainly cortical actin filaments.

Images were collected with a CLSM on a Zeiss LSM510 META with 40X oil objective or on an OLYMPUS fv1000. To reconstruct the 3D images, 100 cross-section images from top to bottom per sample were acquired (LSM image browser, Zeiss, Germany). The focus interval depended on the sample (from 0.5 to 1.2 µm). The resulting stacks were then exported to raw image series or to 3D image data for database integration. Lastly, these stacks were converted into FLASH format and integrated into the database TunicAnatO.

Histology

For histology, *C. robusta* adults were obtained from the Lagoon of Venice, Italy. After *in vitro* fertilization, larvae, metamorphosing individuals, and juveniles were fixed in 1.5% glutaraldehyde buffered with 0.2 M sodium cacodylate, pH 7.4, plus 1.6 % NaCl. After being washed in buffer and postfixated in 1% OsO_4 in 0.2 M cacodylate buffer, specimens were dehydrated and embedded in Araldite. Sections (1 µm) were counterstained with Toluidine blue. Transverse, frontal, and sagittal serial sections were cut. Images were recorded with a digital camera (Leica DFC 480) mounted on a Leica DMR compound microscope. All photos were typeset in Corel Draw X5.

AO/DO ID curation section

The anatomical and developmental terms with synonyms, definitions, and information about developmental events and anatomical entities were accumulated from textbooks, journals, and scientific observations. This information has been collected and formatted in two Excel files: one file on anatomy, the other on development. TunicAnatO was built in OBO format by using the open-source graphical ontology editor OBO-edit ([24]).

List of abbreviations

ADO: Anatomical Developmental Ontology

AO: Anatomical Ontology

ASNET: Ascidian Dendritic Network in Tunic

CLSM: Confocal Scanning Laser Microscopy

DCEN: Dorsal Caudal Epidermal Neurons

DO: Developmental Ontology

ID: Identification

OBO: Open Biological and Biomedical Ontologies

RTEN: Rostral Tail Epidermal Neurons

TunicAnatO: Tunicate Anatomical developmental Ontology

VCEN: Ventral Caudal Epidermal Neurons

Declarations

Ethics approval and consent to participate

Not applicable

Consent for publication

Not applicable

Availability of data and material

The datasets generated and/or analyzed during the current study are available in the following repositories, as well as our database, TunicAnatO (https://www.bpni.bio.keio.ac.jp/tunicanato/top.html).

- Tunicate portal: https://tunicate-portal.org/resources/standards

- Bioportal: https://bioportal.bioontology.org/ontologies/CIROBUADO

- ANISEED: https://www.aniseed.cnrs.fr/aniseed/download/download_data

- FAIRsharing: https://fairsharing.org/bsg-s001475/

Competing interests

The authors declare that they have no competing interests.

Funding

This work was supported by Keio Gijuku Academic Development/ KLL Funds and JSPS KAKENHI Grant Numbers JP16H01451/JP16K07426 to KH, and by the grant "Iniziative di Cooperazione Universitaria 2016", University di Padova, to LM.

Authors' contributions

KH performed CLSM and time-lapse imaging, and constructed the website FABA2 and the database TunicAnatO. LM performed histology. KH and LM analyzed the microscopy images, described the development process, designed and built up the ontology, and drafted the paper. DD implemented entities into the OBO foundation. All participated in revising the manuscript. All authors read and approved the final manuscript.

Acknowledgments

Authors thank the Yutaka Satou Lab at Kyoto University and the Manabu Yoshida Lab at the University of Tokyo and Onagawa Marine Station for providing individuals of *Ciona robusta* with support by the National Bio-Resource Project of AMED, Japan; Akitsu Fukuzawa for collection of CLSM image stacks; Paolo Burighel for the excellent comments and suggestions regarding the ontology.

Figure legends

Figure 1. Methodological procedure to produce the ontology.

A. Gametes were collected from adult individuals of *C. robusta* (Scale bar 2 cm) for *in vitro* fertilization. At a specific time, samples were observed via stereomicroscope, photographed, and fixed for CLSM and histology. **B.** Summary of Stages 26-37. Stereomicroscopy - *in vivo* specimens. Dotted lines in individuals belonging to Stages 34-36 (Body Axis Rotation Period) indicate the angle of rotation. In an individual at Stage 37 (Juvenile Period), the rotation is almost completed and the two axes are almost parallel to each other. Stages 26-33: anterior at left, left view; Stages 34-37: oral siphon (anterior) indicated by arrowhead; left view. Scale bar 100 µm. **C.** After definition of the developmental stages, specimens and literature were analyzed. After that, entities in hierarchical order, definitions, synonyms, developmental information, and literature were annotated in an Excel file. These data were edited using OBO-Edit (http://oboedit.org/), allowing for the visualization of relationships among entities. **D.** Lastly, data were associated with images and movies in the web-based resource TunicAnatO (https://www.bpni.bio.keio.ac.jp/tunicanato/top.html).

Figure 2. Early swimming larva (Stage 27).

A. Larva, dorsal view. Lines on the larval trunk labeled by C-C^{III} and D-D^{III} indicate levels of sagittal and transverse sections shown in C-C^{III} and D-D^{III}, respectively. CLSM. **B-D^{III}**. Selected sections from complete datasets of serially sectioned larvae. B-B^{III} frontal sections from the dorsal to ventral sides; C-C^{III} sagittal sections from the right to left sides; D-D^{III} transverse sections from the anterior to posterior sides. Light microscopy, Toluidine blue. Enlargements in B^{I}-B^{III}, C^{I}-C^{III}, and D^{I}-D^{III} are the same as in B, C, and D, respectively. Green: ectodermal non-neural tissues; yellow: endodermal tissues; light blue: ectodermal neural tissues; dark blue: mesodermal tissues. **E-E^{II}.** Frontal (E), sagittal (E^{I}), and transverse (E^{II}) optic sections of the same larva. CLSM. Enlargement is the same in E-E^{II}. For used symbols, see B-D^{III}. ant pha: anterior pharynx; epi: epidermis; esp: endostyle primordium; est: endodermal strand; lasp: left atrial siphon primordium; mech: mesenchyme; nc: nerve cord; nd: neurohypophyseal duct; ne: neck; noto: notochord; oc: ocellus; osp: oral siphon primordium; ot: otolith; pha: pharynx; post pha: posterior pharynx; pp: papilla; rasp: right anterior siphon primordium; RTEN: cilium of a rostral trunk epidermal neuron; sv: sensory vesicle; tc: test cell; tf: tail fin; vg: visceral ganglion.

Figure 3. Adhesion (Stage 30).

A-A^{II}. Trunk (A), tail tip (A^{I}), and larva (A^{II}) in adhesion, seen from the left side. CLSM. Lines on the larval trunk labeled by C-C^{VII} indicate levels of cross-sections shown in C-C^{VII}. Arrowheads in A^{II}: tunic remnant at the tail tip. Enlargement is the same in A-A^{VII}. **B-B^{III}.** A medial sagittal (B) and three frontal (from dorsal to ventral side) (B^{I}-

B^{III}) optic sections of the larval trunk. CLSM. Enlargement is the same in B-B^{III}. **C-C^{VII}.** Eight transverse sections of the same larva (from anterior to posterior side). Light microscopy, Toluidine blue. ATEN, DCEN, RTEN, VCEN: cilium of an anterior trunk, dorsal caudal, rostral trunk, and ventral caudal epidermal neuron, respectively; cor: coronet cells; epi: epidermis; esp: endostyle primordium; esr: endodermal strand; gp: gut primordium; iclt (C2) and oclt (C1): inner (C2) and outer (C1) cuticular layer of the tunic, respectively; ict and oct: inner and outer compartment of the tunic, respectively; lasp: left atrial siphon primordium; mech: mesenchyme; nc: nerve cord; nd: neurohypophyseal duct; ne: neck; noto: notochord; oc: ocellus; ot: otolith; pha lum: pharynx lumen; pl: preoral lobe; pp: ventral papilla; rasp: right atrial siphon primordium; sv: sensory vesicle; tc: test cell; tf: tail fin; vg: visceral ganglion.

Figure 4. Early body axis rotation (Stage 34).

Description of data: A-A^{IV}. Metamorphosing larva seen from the left side (A) and its medial sagittal optic section (A^{I}). In A, note that the body is rotated about 30°. In A^{I}, the area bordered by the red line is enlarged in A^{II}; that one bordered by the black line is enlarged in A^{III}; the line marked by A^{IV} represents the level of section A^{IV}. Enlargement is the same in A-A^{I}, and in A^{II}-A^{IV}. CLSM. B-B^{IV}. Serial sagittal histological section of a metamorphosing larva from the left to right sides (B, B^{II}-B^{IV}); the area bordered by the black line in B is enlarged in B^{I} to show the oral siphon and neural complex. Enlargement is the same in B and B^{II}-B^{IV}. Toluidine blue. brc: branchial chamber; cil duc: ciliated duct of the neural gland; cg: cerebral ganglion; es: endostyle; hc: maemocytes; ht: heart; las: left atrial siphon; int: intestine; lbr: larval brain remnants; ng: neural gland; oes: oesophagus; os; oral siphon; osm: oral siphon muscle; pyc: pyloric caecum; ras: right atrial siphon; stom: stomach; tail remn: tail remnants; tun: tunic; tunc: tunic cells.

Figure 5. Late body axis rotation (Stage 36).

A-A^{II}. Metamorphosing larva, seen from the left side (A), its medial sagittal optic section (A^{I}), and its depth-coded image (A^{II}). The depth information is represented by a heat map: Warmer colors go to the front, and cooler colors to the back. Color bar: value of depth (µm). Confocal microscopy. Enlargement is the same in A-A^{II}. **B-B^{I}.** Two sagittal sections of a metamorphosing larva. In B, lines on the larval trunk, labeled by C and D-D^{III}, indicate levels of the transverse section and the frontal sections shown in C and D-D^{III}, respectively. Asterisks: protostigmata. Toluidine blue. Enlargement is the same in B-B^{I}. **C.** Transverse section of the metamorphosing larva at endostyle and oral siphon level. Note the differentiating eight zones in endostyle (1-8). Toluidine blue. **D-D^{III}.** Serial frontal histological sections of a metamorphosing larva from the dorsal (D) to ventral (D^{III}) sides. Toluidine blue. Enlargement is the same in D-D^{III}. brc: branchial chamber; cil duc: ciliated duct of neural gland; ds: dorsal sinus; dst: dorsal strand; es: endostyle; hc: haemocytes; ht: heart; lbr: larval brain remnant; mi: medium intestine; mc: myocardium; ng: neural gland; oes: oesophagus; os: oral siphon; osm: oral siphon muscle; pb: peripharyngeal band; pc: pericardium; pg: pyloric gland; prox int: proximal intestine; rph: raphe; rpsm: right protostigmata; stom: stomach; tail remn: tail remnants; tun: runic; tunc: tunic cells; ve: velum.

Figure 6. Number variation of anatomical entities in each developmental stage.

Upper part: Matrix showing the variation in number (in ordinate) of anatomical entities during development (Stages in abscissa), from Stage 0 (unfertilized egg) to animal death. Blue columns (cell) refer to entities

recognizable at the cell lineage level; red columns (anato) refer to entities recognizable at the anatomical level (thanks to CLSM and histological data); violet columns (func) refer to the organ functional state. Lower part: table showing the number of entities recognized at the cell level (cell), anatomical level (anato), and functional level (func) in each Stage/Period. U: Stage 0, Unfertilized egg; F: Stage 1, Fertilized egg; 32: Stage 6, 32 cell; 64: Stage 8, 64 cell; Gst: Gastrula Period; Neu: Neurula Period; TB: Tailbud Period; Lv: Larva Period; Ad: Adhesion Period; Absorption: Tail Absorption Period; BodyRotation: Body Rotation Period; Juvenile: Juvenile Period; 2^{nd}: 2^{nd} Ascidian Stage; Adult: Adult Stage; Death: Animal Death.

Tables

Table 1. *C. robusta* developmental stages from the Larva Period to the Juvenile Period. Stages 1-41 were defined in the paper, Stages 1-37 described.

Additional files

Additional file 1

File name: Additional_file_1_Life_Cycle

File format: .jpg

Title of data: Life cycle of *C. robusta*

Description of data: Scheme of the life cycle of *C. robusta*. Blue box: developmental stages described in Hotta et al., 2007. Red box: developmental stages described in this paper.

Additional file 2

File name: Additional_file_2_Movie

File format: .mov

Title of data: *C. robusta* development

Description of data: Time-lapse movie showing the development of *C. robusta* from the fertilized egg (Stage 1) to the juvenile (Stage 38). Observation was performed at 18°C for Stages 1-26 and at 20°C for Stages 26-37.

Additional file 3

File name: Additional_file_3_3D

File format: .tif

Title of data: Three-dimensional reconstructed images of *C. robusta* post hatching stages

Description of data: Specimens labeled with Alexa 546 phalloidine (Molecular Probes). As the staining targets actin filaments, the cortical cytoplasm is stained in each cell. Stages 26-33: left view, anterior (adhesive papillae) at left. Stages 34-37: right view, anterior (oral siphon) at right (Stages 34-35) or top (Stages 36-37). Scale bar: 50 □m. CLSM.

Additional file 4

File name: Additional_file_4_Ciona_Staging_Table

File format: .pdf

Title of data: Table of developmental stages in *C. robusta*

Description of data: Table listing the Meta-Periods, Periods, and Stages of development of *C. robusta*, from Stage 0 (unfertilized egg) to Stage 43 (adult). Main features, time of appearance after fertilization, and comparison with the staging method by Chiba and collaborators (Chiba et al., 2004) are reported for each stage. Yellow: stages defined in this work; Stages 26-37 are described in the present work.

Additional file 5

File name: Additional_file_5_Reference_List

File format: .xls

Title of data: List of references included in the ontology

Description of data: References used to build up and annotate in the AO and the DO of *C. robusta*.

Additional file 6

File name: Additional_file_6_Anatomical_Ontology

File format: .xls

Title of data: Anatomical Ontology of *C. robusta* from Stage 26 to Stage 37

Description of data: Table listing the anatomical entities of the AO (Columns B-F: Terms and their specifications), their definition (Column G), Part of (Column H), Develops from (Column I), End Stage (Column J), Start Stage (Column K), Comment (Column L), Literature (Column M), and ID (Column N).

Additional file 7

File name: Additional_file_7_Anatomical_Dictionary

File format: .xls

Title of data: List of anatomical entities and their definition

Description of data: Table listing, in alphabetical order, the anatomical entities of the AO, their abbreviations used in Figures and Additional files, and their definitions.

Additional file 8

File name: Additional_file_8_Stage_26

File format: .jpg

Title of data: Hatching larva (Stage 26). CLSM

Description of data: **A.** Larva. DCEN, RTEN, VCEN: cilia to dorsal caudal, rostral trunk, and ventral caudal epidermal neurons, respectively; pp: three anterior adhesive papillae. **B-B^{I}.** Medial sagittal optic sections of the larval trunk (B) and posterior part of the tail (B^{I}). Enlargement is the same in B and B^{I}. **C-C^{I}.** Transverse optic sections of larval trunk at sensory vesicle (C) and the atrial siphon primordia (C^{I}) level. Enlargement is the same in C and C^{I}. **D-D^{I}.** Frontal optic sections of the larval trunk at the sensory vesicle (D) and ventral pharynx (D^{I}) level. Enlargement is the same as C. ant pha: anterior pharynx; CNS: larval central nervous system; epi: epidermis; lasp: left atrial siphon primordium; mech: mesenchyme; ne: neck; nc: nerve cord; noto: notochord; oc: ocellus; osp: oral siphon primordium; noto: notochord; pha: pharynx; post pha: posterior pharynx; pp: papilla; rasp: right atrial siphon primordium; sv: sensory vesicle; vg: visceral ganglion.

Additional file 9

File name: Additional_file_9_Stage_28

File format: .jpg

Title of data: Mid swimming larva (Stage 28)

Description of data: **A.** Larva, left view. Note the ciliary network belonging to the epidermal sensory neurons (DCEN, RTEN, VCEN: cilium of a dorsal caudal, rostral trunk, and ventral caudal epidermal neuron, respectively). CLSM. **B.** Median sagittal optic section. CLSM. **C-C^{II}.** Three selected sagittal sections from a complete dataset of a serially sectioned larva from left (C) to right (C^{II}). Light microscopy, Toluidine blue. **D-D^{I}.** Two transverse optic sections of the same larva of B. Enlargement is the same in D-D^{I}. CNS: central nervous system; cor: coronet cells; epi: epidermis; ict: inner compartment of tunic; iclt (C2): inner cuticular layer of the tunic (C2); lasp: left oral siphon primordium; mech: mesenchyme; nc: nerve cord; nd: neurohypophyseal duct; ne: neck; noto: notochord; pl: preoral lobe; oclt (C1): outer cuticular layer of the tunic (C1); oct: outer compartment of the tunic; oct/tf: outer compartment of the tunic/tail fin; osp: oral siphon primordium; pha: pharynx; pp: dorsal papillae; sv: sensory vesicle; vg: visceral ganglion.

Additional file 10

File name: Additional_file_10_Stage_29

File format: .jpg

Title of data: Late swimming larva (Stage 29)

Description of data: **A.** Larva, left view. CLSM. ATEN, DCEN, RTEN, VCEN: cilium of an anterior trunk, dorsal caudal, rostral trunk, and ventral caudal epidermal neuron, respectively. **B.** Medial sagittal optic section of the larval trunk. CLSM. **C-C^{I}.** Two frontal sections of the same larva, at the level of atrial siphon primordia (C) and endodermal strand (esr) (C^{I}). Light microscopy, Toluidine blue. Enlargement is the same in C-C^{I}. **D-D^{VII}.** Eight selected transverse sections from a complete dataset of a serially sectioned larva from anterior (D) to posterior (D^{VII}). Light microscopy, Toluidine blue. Enlargement is the same in D-D^{VII}. CNS: central nervous system; cor: coronet cells; epi: epidermis; esp: endostyle primordium; iclt (C2) and oclt (C1): inner (C2) and outer (C1) cuticular layer of the tunic, respectively; gp: gut primordium; lasp: left atrial siphon primordium; mech: mesenchyme; nc: nerve cord; noto: notochord; oc: ocellus; ot: otolith; pha lum: pharynx lumen; pl: preoral lobe; pp: ventral papilla; rasp: right atrial siphon primordium; sv: sensory vesicle; tc: test cell; tf: tail fin; tmc: tail muscle cells; tun: tunic; tunc: tunic cells; vg: visceral ganglion.

Additional file 11

File name: Additional_file_11_Stages_31-32

File format: .jpg

Title of data: Early tail absorption (Stage 31) (A-B^{I}) and mid tail absorption (Stage 32) (C-F^{III}). CLSM

Description of data: **A.** Larva in early tail absorption, seen from the left side. **B-B^{I}.** Medial sagittal optic sections of the trunk (B) and tail tip (B^{I}) of the larva shown in A. **C.** Larva in the mid-tail absorption, seen from the left side. The line on the larval trunk labeled by D^{II} indicates the level of the transverse section shown in D^{II}. **D-D^{I}.** Medial sagittal optic sections of the tail tip (D) and trunk (D^{I}) of the larva shown in C. In D^{I}, the line on the larval trunk labeled by D^{II} indicates the level of transverse section shown in D^{II}. Enlargement is the same in D-D^{I}. **D^{II}.** Transverse optic section of the larval trunk shown in C and D^{II}. **E-E^{II}.** Larva in mid-tail absorption (E), seen from the left side, at a slightly more advanced stage than in C, and detail of its tail tip (E^{I}, and its optic section in E^{II}). The lines on the larval trunk labeled by F and F^{II} indicate the levels of sections shown in F and F^{II}, respectively. Enlargement is the same in E-E^{II}. **F-F^{II}.** Transverse (F), medial sagittal (F^{I}), and frontal (F^{II}) optic sections of the trunk of larva shown in E. Enlargement is the same in F^{I}-F^{II}. abs tail: absorbing tail; ATEN, DCEN, RTEN, VCEN: cilium of an anterior trunk, dorsal caudal, rostral trunk, and ventral caudal epidermal neuron, respectively; deg pp: degenerating papilla; deg tail: degenerating tail; esr: endodermal strand; epi: epidermis; esp: endostyle primordium; gp: gut primordium; ht: heart; lasp: left atrial siphon primordium; lbr: larval brain remnants; mech: mesenchyme; oes: oesophagus; ne: neck; noto: notochord; pha lum: pharynx lumen; pl: preoral lobe; pp: ventral papilla; rasp: right atrial siphon primordium; sv: sensory vesicle; tf: tail fin; tmc: tail muscle cell; tunc: tunic cells; vg: visceral ganglion.

Additional file 12

File name: Additional_file_12_Stage_33

File format: .jpg

Title of data: Late tail absorption (Stage 33). CLSM

Description of data: **A-A^{II}.** Larva in late tail adsorption (A), seen from the dorsal side, and optic frontal (A^{I}) and transverse (A^{II}) sections. The line on the larval trunk labeled by A^{II} indicates the level of the section shown in A^{II}.

Enlargement is the same in A-A^{I}. **B-B^{II}.** Larva in late tail absorption (B), seen from the dorsal side at a more advanced stage than in A, and optic frontal (B^{I}) and transverse (B^{II}) sections. The line on the larval trunk labeled by B^{II} indicates the level of the section shown in B^{II}. Enlargement in B-B^{I} is the same as in A. abs tail: absorbing tail; brc: branchial chamber; esp: endostyle primordium; gp: gut primordium; gs: gill slit; hc: haemocyte; lasp: left atrial siphon primordium; os: oral siphon; rasp: right atrial siphon primordium.

Additional file 13

File name: Additional_file_13_Stage_35

File format: .jpg

Title of data: Mid body axis rotation (Stage 35)

Description of data: **A-A^{IV}.** Metamorphosing larva, seen from the left side (A) and its medial sagittal (A^{I}), frontal (A^{II}), and transverse (A^{III}) optic sections. A^{IV} is an enlargement of the squared area in A^{I}. In A^{I}, the lines on the larval trunk labeled by A^{II} and A^{III} indicate the levels of sections shown in A^{II} and A^{III}, respectively. brc: branchial chamber; cil duc: ciliated duct of neural gland; es: endostyle; hc: haemocytes; ht: heart; las: left atrial siphon; lpsm: left protostigmata; ng: neural gland; os: oral siphon; osm: oral siphon muscle; psm: right protostigmata; stom: stomach; tail remn: tail remnants; tun: runic; tunc: tunic cells. Enlargement is the same in A and A^{I}.

Additional file 14

File name: Additional_file_14_Stage_37.pdf

File format: .jpg

Title of data: Early juvenile I (Stage 37)

Description of data: **A-A^{II}.** Juvenile, seen from the left side (A), its medial sagittal optic section (A^{I}) and its depth-coded image. The depth information is represented by a heat map: warmer colors go to the front, and cooler colors to the back. For the color bar, see A^{II}. Lines indicated by B-B^{VI} in A represent the level of transverse sections shown in B-B^{VI}. Confocal microscopy. Enlargement is the same in A-A^{II}. **B-B^{VI}.** Transverse sections of a juvenile from the dorsal (B) to ventral (B^{VI}) sides. Squared areas in B^{III} and B^{IV} are enlarged in insets to show details of endostyle (B^{III}), left atrial siphon (black square), and row of ciliated cells of a protostigma (red square) (B^{IV}), respectively. Numbers 1-8 in the inset of B^{III} indicate the eight zones of endostyle. Arrowheads in B^{II}: ciliated cells of the coronal organ; asterisks in B^{III}-B^{IV}: protostigmata. Toluidine blue. Enlargement is the same in B-B^{VI}. as: atrial siphon; brc: branchial chamber; cil duc: ciliated duct of neural gland; cg: cerebral ganglion; cut: tunic cuticle; dl: dorsal lamina; es: endostyle; hc: haemocyte; int: intestine; las: left atrial siphon; lasm: left atrial siphon muscles; lbr: larval brain remnant; man: mantle; mc: myocardium; mint: medium intestine; ng: neural gland; oes: oesophagus; os: oral siphon; osm: oral siphon muscle; pb: peripharyngeal band; pc: pericardium; pg: pyloric gland; prox int: proximal intestine; psm: protostigmata; pyc: pyloric caecum; stom: stomach; term int: terminal intestine, close to anus; ras: right atrial siphon; tail remn: tail remnants; ten: oral tentacles; tun: runic; tunc: tunic cells.

Additional file 15

File name: Additional_file_15_start-end_matrix

File format: .pdf

Title of data: Start-end matrix of anatomical entities

Description of data: Upper matrix: part of lower matrix showing, for each anatomical entity (listed in ordinate), the *Start stage* and *End stage* (Stages in abscissa). Cells in light yellow show the stages in which an entity is recognizable at the cell lineage level (cell); those in dark yellow show the stages in which an entity is recognizable at the anatomical level (thanks to CLSM and histological data) (anato); those in brown show the stages in which an entity is recognizable at the functional level (func). In the lower matrix, the light blue square highlights 111 entities (such as the epidermis, inner compartment of the tunic, tunic cells) recognizable during embryogenesis but not eliminated at metamorphosis; blue squares highlight larval 88 entities (starting during embryogenesis but resorbed during metamorphosis); yellow squares highlight 93 juvenile/adult entities formed during metamorphosis for adult life. U: Stage 0, Unfertilized egg; F: Stage 1, Fertilized egg; 32: Stage 6, 32 cell; 64: Stage 8, 64 cell; Gst: Gastrula Period; Neu: Neurula Period; TB: Tailbud Period; Lv: Larva Period; Ad: Adhesion Period; Absorption: Taail Absorption Period; BodyRotation: Body Rotation Period; Juvenile: Juvenile Period; 2^{nd}: 2^{nd} Ascidian Stage; adult: Adult Stage; Death: Animal Death.

Additional file 16

File name: Additional_file_16_available_ontologies

File format: .jpg

Title of data: List of anatomical ontologies

Description of data: Table of ontologies regarding the anatomy of animal model organisms summarizing: the combination of AO with developmental stages, the number of anatomical terms listed, the percentage number of the relation “develops from” with respect to the total number of terms, the use of references as a source of data, and the link to the FAIRsharing database.

1. Van Slyke CE, Bradford YM, Westerfield M, Haendel MA. The zebrafish anatomy and stage ontologies: representing the anatomy and development of Danio rerio. J Biomed Semantics. 2014;5:12. doi:10.1186/2041-1480-5-12.

2. Richardson L, Armit C. Digital Graphical Resources and Developmental Anatomy in the Mouse. In: Kaufman’s Atlas of Mouse Development Supplement. 2016.

3. Mungall CJ, Torniai C, Gkoutos G V., Lewis SE, Haendel MA. Uberon, an integrative multi-species anatomy ontology. Genome Biol. 2012;13:R5. doi:10.1186/gb-2012-13-1-r5.

4. Manni L, Gasparini F, Hotta K, Ishizuka KJ, Ricci L, Tiozzo S, et al. Ontology for the asexual development and anatomy of the colonial chordate botryllus schlosseri. PLoS One. 2014;9.

5. Segerdell E, Ponferrada VG, James-Zorn C, Burns K a, Fortriede JD, Dahdul WM, et al. Enhanced XAO: the ontology of Xenopus anatomy and development underpins more accurate annotation of gene expression and queries on Xenbase. J Biomed Semantics. 2013;4:31. doi:10.1186/2041-1480-4-31.

6. Bourlat SJ, Juliusdottir T, Lowe CJ, Freeman R, Aronowicz J, Kirschner M, et al. Deuterostome phylogeny reveals monophyletic chordates and the new phylum Xenoturbellida. Nature. 2006.

7. Delsuc F, Brinkmann H, Chourrout D, Philippe H. Tunicates and not cephalochordates are the closest living relatives of vertebrates. Nature. 2006.

8. Brunetti R, Gissi C, Pennati R, Caicci F, Gasparini F, Manni L. Morphological evidence that the molecularly determined Ciona intestinalis type A and type B are different species: Ciona robusta and Ciona intestinalis. J Zool Syst Evol Res. 2015;53:186–93. doi:10.1111/jzs.12101.

9. Pennati R, Ficetola GF, Brunetti R, Caicci F, Gasparini F, Griggio F, et al. Morphological differences between larvae of the Ciona intestinalis species complex: Hints for a valid taxonomic definition of distinct species. PLoS One. 2015.

10. Gissi C, Hastings KEM, Gasparini F, Stach T, Pennati R, Manni L. An unprecedented taxonomic revision of a model organism: the paradigmatic case of Ciona robusta and Ciona intestinalis. Zoologica Scripta. 2017.

11. Satoh N. The ascidian tadpole larva: Comparative molecular development and genomics. Nat Rev Genet. 2003;4:285–95. doi:10.1038/nrg1042.

12. Corbo JC, Di Gregorio A, Levine M. The Ascidian as a Model Organism in Developmental and Evolutionary Biology. Cell. 2001;106:535–8. doi:10.1016/S0092-8674(01)00481-0.

13. Procaccini G, Affinito O, Toscano F, Sordino P. A New Animal Model for Merging Ecology and Evolution. In: Evolutionary Biology – Concepts, Biodiversity, Macroevolution and Genome Evolution. Berlin, Heidelberg: Springer Berlin Heidelberg; 2011. p. 91–106. doi:10.1007/978-3-642-20763-1_6.

14. Gallo A, Tosti E. The Ascidian Ciona Intestinalis as Model Organism for Ecotoxicological Bioassays. J Mar Sci Res Dev. 2015.

15. Hotta K, Mitsuhara K, Takahashi H, Inaba K, Oka K, Gojobori T, et al. A web-based interactive developmental table for the Ascidian Ciona intestinalis, including 3D real-image embryo reconstructions: I. From fertilized egg to hatching larva. Dev Dyn. 2007;236:1790–805.

16. Whetzel PL, Noy NF, Shah NH, Alexander PR, Nyulas C, Tudorache T, et al. BioPortal: Enhanced functionality via new Web services from the National Center for Biomedical Ontology to access and use ontologies in software applications. Nucleic Acids Res. 2011.

17. Conklin EG. Mosaic development in ascidian eggs. J Exp Zool. 1905;2:145–223. doi:10.1002/jez.1400020202.

18. Nishida H. Cell Lineage Analysis in Ascidian Embryos by Intracellular Injection of a Tracer Enzyme III. Up to the Tissue Restricted Stage. Dev Biol. 1987;121:526–41.

19. Nishida H, Satoh N. Cell Lineage Analysis in Ascidian Embryos by Intracellular Injection of a Tracer Enzyme I. Up to the Eight-Cell Stage. Dev Biol. 1983;99:382–94.

20. Satoh N. CELLULAR MORPHOLOGY AND ARCHITECTURE DURING EARLY MORPHOGENESIS OF THE ASCIDIAN EGG: AN SEM STUDY. Biol Bull. 1978;155:608–14.

21. CLONEY RA. Ascidian Larvae and the Events of Metamorphosis. Am Zool. 1982;22:817–26. doi:10.1093/icb/22.4.817.

22. R. H. Millar. XXXV. CIONA. In: L.M.B.C. 1953. p. 1–123.

23. Chiba S, Sasaki A, Nakayama A, Takamura K, Satoh N. Development of Ciona intestinalis juveniles (through 2nd ascidian stage). Zoolog Sci. 2004;21:285–98.

24. Day-Richter J, Harris MA, Haendel M, Lewis S. OBO-Edit an ontology editor for biologists. Bioinformatics. 2007;23:2198–200. doi:10.1093/bioinformatics/btm112.

25. Taniguchi K, Nishida H. Tracing cell fate in brain formation during embryogenesis of the ascidian Halocynthia roretzi. Dev Growth Differ. 2004;46:163–80.

26. Hudson C. The central nervous system of ascidian larvae. Wiley Interdiscip Rev Dev Biol. 2016;5:538–61. doi:10.1002/wdev.239.

27. Hirano T, Nishida H. Developmental fates of larval tissues after metamorphosis in the ascidian, Halocynthia roretzi. II. Origin of endodermal tissues of the juvenile. Dev Genes Evol. 2000;210:55–63. doi:10.1007/s004270050011.

28. Nakazawa K, Yamazawa T, Moriyama Y, Ogura Y, Kawai N, Sasakura Y, et al. Formation of the digestive tract in Ciona intestinalis includes two distinct morphogenic processes between its anterior and posterior parts. Dev Dyn. 2013;242:1172–83. doi:10.1002/dvdy.24009.

29. Imai J, Meinertzhagen IA. Neurons of the Ascidian Larval Nervous System in Ciona intestinalis: I. Central Nervous System. J Comp Neurol. 2007;501:316–34.

30. Ryan K, Lu Z, Meinertzhagen IA. The CNS connectome of a tadpole larva of Ciona intestinalis (L.) highlights sidedness in the brain of a chordate sibling. Elife. 2016;5:1–34. doi:10.7554/eLife.16962.

31. Moret F, Christiaen L, Deyts C, Blin M, Joly JS, Vernier P. The dopamine-synthesizing cells in the swimming larva of the tunicate Ciona intestinalis are located only in the hypothalamus-related domain of the sensory vesicle. Eur J Neurosci. 2005;21:3043–55.

32. Razy-Krajka F, Brown ER, Horie T, Callebert J, Sasakura Y, Joly JS, et al. Monoaminergic modulation of photoreception in ascidian: evidence for a proto-hypothalamo-retinal territory. BMC Biol. 2012;10:45. doi:10.1186/1741-7007-10-45.

33. Horie T, Horie R, Chen K, Cao C, Nakagawa M, Kusakabe TG, et al. Regulatory cocktail for dopaminergic neurons in a protovertebrate identified by whole-embryo single-cell transcriptomics. Genes Dev. 2018;32:1297–302.

34. Parrinello D, Parisi M, Parrinello N, Cammarata M. Ciona robusta hemocyte populational dynamics and PO-dependent cytotoxic activity. Dev Comp Immunol. 2020;103 May 2019:103519. doi:10.1016/j.dci.2019.103519.

35. Bostwick M, Smith EL, Borba C, Newman-Smith E, Guleria I, Kourakis MJ, et al. Antagonistic Inhibitory Circuits Integrate Visual and Gravitactic Behaviors. Curr Biol. 2020;:1–10. doi:10.1016/j.cub.2019.12.017.

36. Wakai MK, Nakamura MJ, Sawai S, Hotta K, Oka K. Two-Round Ca2+ Transients in Papillae by Mechanical Stimulation Induces Metamorphosis in the Ascidian,. 2020.

37. Matsunobu S, Sasakura Y. Time course for tail regression during metamorphosis of the ascidian Ciona intestinalis. Dev Biol. 2015;405:71–81. doi:10.1016/j.ydbio.2015.06.016.

38. Cloney RA. Cytoplasmic filaments and morphogenesis: effects of cytochalasin B on contractile epidermal cells. Zellforsch. 1972;132:167–92.

39. Numakunai T. Hentai. In: Japan TZS of, editor. Gendai Doubutsugaku No Kadai vol.5. Gakkai Shuppan Center; 1977. p. 135–75. https://www.amazon.co.jp/現代動物学の課題-5-変態-日本動物学会/dp/4762200808.

40. Karaiskou A, Swalla BJ, Sasakura Y, Chambon J-PP. Metamorphosis in solitary ascidians. Genesis. 2015;53:34–47. doi:10.1002/dvg.22824.

41. Lash JW, Cloney RA, Minor RR. The effect of cytochalasin B upon tail resorption and metamorphosis in ten species of ascidians. Biol Bull. 1973;145:360–72. doi:10.2307/1540046.

42. Terakubo HQ, Nakajima Y, Sasakura Y, Horie T, Konno A, Takahashi H, et al. Network structure of projections extending from peripheral neurons in the tunic of ascidian larva. Dev Dyn. 2010;239:2278–87. doi:10.1002/dvdy.22361.

43. Hirano T, Nishida H. Developmental Fates of Larval Tissues after Metamorphosis in AscidianHalocynthia roretzi. Dev Biol. 1997;192:199–210. doi:10.1006/dbio.1997.8772.

44. Davidson B. Ciona intestinalis as a model for cardiac development. Semin Cell Dev Biol. 2007;18:16–26. doi:10.1016/j.semcdb.2006.12.007.

45. Davidson B, Levine M. Evolutionary origins of the vertebrate heart: Specification of the cardiac lineage in Ciona intestinalis. Proc Natl Acad Sci U S A. 2003;100:11469–73. doi:10.1073/pnas.1634991100.

46. Stolfi A, Gainous TB, Young JJ, Mori A, Levine M, Christiaen L. Early Chordate Origins of the Vertebrate Second Heart Field. Science (80-). 2010;329:565. doi:10.1126/science.202625.

47. Wang W, Razy-Krajka F, Siu E, Ketcham A, Christiaen L. NK4 Antagonizes Tbx1/10 to Promote Cardiac versus Pharyngeal Muscle Fate in the Ascidian Second Heart Field. PLoS Biol. 2013;11:e1001725. doi:10.1371/journal.pbio.1001725.

48. Burighel P, Cloney RA, Cloney B. Microscopic Anatomy of Invertebrates, Vol. 15. Microsc Anat Invertebr. 1997;15:221–347. http://www.nhbs.com/title/53150/microscopic-anatomy-of-invertebrates-volume-15. Accessed 9 May 2017.

49. Kawamura K, Tiozzo S, Manni L, Sunanaga T, Burighel P, De Tomaso AW. Germline cell formation and gonad regeneration in solitary and colonial ascidians. Dev Dyn. 2011;240:299–308.

50. Shirae-Kurabayashi M, Nishikata T, Takamura K, Tanaka KJ, Nakamoto C, Nakamura A. Dynamic redistribution of vasa homolog and exclusion of somatic cell determinants during germ cell specification in Ciona intestinalis. Development. 2006;133:2683–93. doi:10.1242/dev.02446.

51. Stolfi A, Lowe EK, Racioppi C, Ristoratore F, Brown CT, Swalla BJ, et al. Divergent mechanisms regulate conserved cardiopharyngeal development and gene expression in distantly related ascidians. Elife. 2014;3:e03728.

52. Hozumi A, Horie T, Sasakura Y. Neuronal map reveals the highly regionalized pattern of the juvenile central nervous system of the ascidian Ciona intestinalis. Dev Dyn. 2015;244:1375–93.

53. Mackie GO, Burighel P, Caicci F, Manni L. Innervation of ascidian siphons and their responses to stimulation. Can J Zool. 2006;84:1146–62. doi:10.1139/z06-106.

54. Manni L, Agnoletto A, Zaniolo G, Burighel P. Stomodeal and neurohypophysial placodes in Ciona Intestinalis: insights into the origin of the pituitary gland. J Exp Zool Part B Mol Dev Evol. 2005;304B:324–39. doi:10.1002/jez.b.21039.

55. Veeman MT, Newman-Smith E, El-Nachef D, Smith WC. The ascidian mouth opening is derived from the anterior neuropore: reassessing the mouth/neural tube relationship in chordate evolution. Dev Biol. 2010;344:138–49. doi:10.1016/j.ydbio.2010.04.028.

56. Ogasawara M, Satoh N. Isolation and Characterization of Endostyle-Specific Genes in the Ascidian Ciona intestinalis a:::: supporting elements. World Wide Web Internet Web Inf Syst. 1998;:60–9.

57. Chambon J-PP, Soule J, Pomies P, Fort P, Sahuquet A, Alexandre D, et al. Tail regression in Ciona intestinalis (Prochordate) involves a Caspase-dependent apoptosis event associated with ERK activation. Development. 2002;129:3105–14.

58. Willey A. Memoirs: Studies on the Protochordata. Quart J Micr Sci. 1893;s2-34:317–60. http://jcs.biologists.org/content/s2-34/135/317.abstract. Accessed 15 Apr 2020.

59. Kott P. The Australian Ascidiacea. Part 1, Phlebobranchia and Stolidobranchia. Mem Queensl Museum. 1985.

60. Stolfi A, Ryan K, Meinertzhagen IA, Christiaen L. Migratory neuronal progenitors arise from the neural plate borders in tunicates. Nature. 2015;527:371–4. doi:10.1038/nature15758.

61. Jeffery WR, Chiba T, Krajka FR, Deyts C, Satoh N, Joly JS. Trunk lateral cells are neural crest-like cells in the ascidian Ciona intestinalis: Insights into the ancestry and evolution of the neural crest. Dev Biol. 2008;324:152–60. doi:10.1016/j.ydbio.2008.08.022.

62. Abitua PB, Wagner E, Navarrete IA, Levine M. Identification of a rudimentary neural crest in a non-vertebrate chordate. Nature. 2012;492:104–7. doi:10.1038/nature11589.

63. Nishida H, Satoh N. Cell lineage analysis in ascidian embryos by intracellular injection of a tracer enzyme. II. The 16- and 32-Cell Stages. Dev Biol. 1985;110:440–54.

64. Nakamura MJ, Terai J, Okubo R, Hotta K, Oka K. Three-dimensional anatomy of the Ciona intestinalis tailbud embryo at single-cell resolution. Dev Biol. 2012;372:274–84. doi:10.1016/j.ydbio.2012.09.007.

65. Sansone S-A, McQuilton P, Rocca-Serra P, Gonzalez-Beltran A, Izzo M, Lister AL, et al. FAIRsharing as a community approach to standards, repositories and policies. Nat Biotechnol. 2019;37:358–67. doi:10.1038/s41587-019-0080-8.

66. Essock-Burns T, Gohad N V., Orihuela B, Mount AS, Spillmann CM, Wahl KJ, et al. Barnacle biology before, during and after settlement and metamorphosis: a study of the interface. J Exp Biol. 2017;220:194–207. doi:10.1242/jeb.145094.

67. Kitamura H, Kitahara S, Koh HB. The induction of larval settlement and metamorphosis of two sea urchins, Pseudocentrotus depressus and Anthocidaris crassispina, by free fatty acids extracted from the coralline red alga Corallina pilulifera. Mar Biol. 1993;115:387–92. doi:10.1007/BF00349836.

Table 1. Ciona intestinalis developmental stages from hatching to juvenile.

Stage	Stage name	Characteristics	Time after fertilization
Embryonic development, pre-metamorphosis			
CirobuD:0000003			
VI. Larva Period (St.26~29, 17.5~24hpf)			
St. 26 CirobuD:0000049	hatching larva	Hatching, spherical head shape, immature papillae with pyramidal shape, irregular tail movements	17hr 30min (17.5hpf)
St. 27 CirobuD:0000050	early swimming larva	Spindle-like head shape, regular tail movements and swimming behaviour	17.5-20 hpf
St. 28 CirobuD:0000051	mid swimming larva	Elongated papillae and expansion of their basal part, squared head, spherical test cells, cilia in epidermal sensory neurons recognizable, preoral lobe recognizable	20-22hpf
St. 29 CirobuD:0000052	late swimming larva	Longer and narrower head with respect to St. 28, trunk profile squared at transition between trunk and tail	22-24hpf
Metamorphosis			
CirobuD:0000004			
VII. Adhesion period (St.30~31, 24~27hpf)			
St. 30 CirobuD:0000053	adhesion	Curved papillae, otolith and ocellus remnants recognizable	24-27 hpf
VIII.Tail absorption period (St.32~34, 27~30hpf)			
St. 31 CirobuD:0000054	early tail absorption	Beginnng of tail absorption, tail bending at the transition between trunk and tail, otolith and ocellus remnants recognizable.	27 hpf
St. 32 CirobuD:0000055	mid tail absorption	50% of tail absorbed into trunk; tail shrinked and thickened, otolith and ocellus remnants recognizable	28 hpf
St. 33 CirobuD:0000056	late tail absorption	Tail completely resorbed, papiliae no more recognizable, otolith and ocellus remnants recognizable	29 hpf
IX. Body axis rotation period (St.35~37, 30~60hpf)			
St. 34 CirobuD:0000057	early body axis rotation	Beginning of body axis rotation (angle between the stalk and the endostyle more than 0°), outer tunic compartment and outer cuticle layer no more present, tunic cells recognizable in definitive tunic, otolith and ocellus remnants recognizable.	30-36 hpf
St. 35 CirobuD:0000058	mid body axis rotation	Body axis rotation of about 30°-60°, one pair of gill-slit recognizable, otolith and ocellus remnants recognizable	36-45 hpf
St. 36 CirobuD:0000059	late body axis rotation	Two pairs of gill-slit open, body axis rotation of about 80°-90°, filtering and feeding activity present, otolith and ocellus remnants recognizable, heart beating	45-60 hpf (2dpf)
Post-metamorphosis			
CirobuD:0000005			
X. Juvenile period (St.37-41, 60hpf~)			
St. 37 CirobuD:0000060	early juvenile I	Body axis rotation completed, stomach swollen, otolith and ocellus remnants recognizable	63-72 hpf (3dpf)
St. 38 CirobuD:0000061	early juvenile II	Larval tail remnants totally adsorbed	4 dpf
St. 39 CirobuD:0000062	mid juvenile I	Additional gill slit begin to open, appearance of stomach, gut and neural grand	6 dpf
St.40 CirobuD:0000063	mid juvenile II	Gonad in form of oval vesicle (corresponding to Stage 6 in Chiba et. al., 2004)	7dpf
St.41 CirobuD:0000064	late juvenile	Atrial siphon begins to fuse (corresponding to Stage 7 in Chiba et. al., 2004)	7dpf~

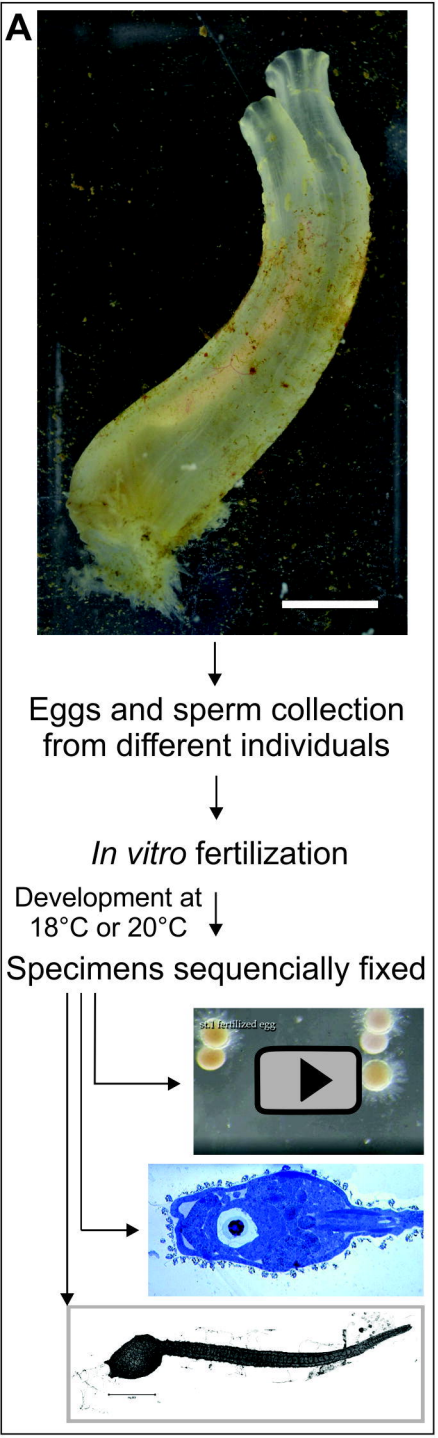

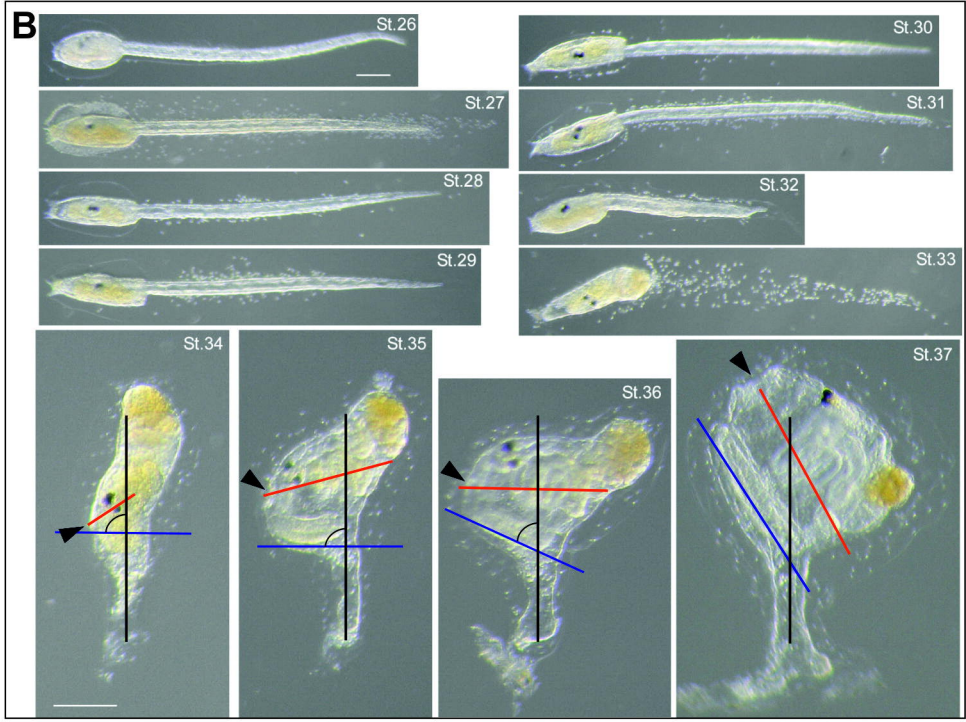

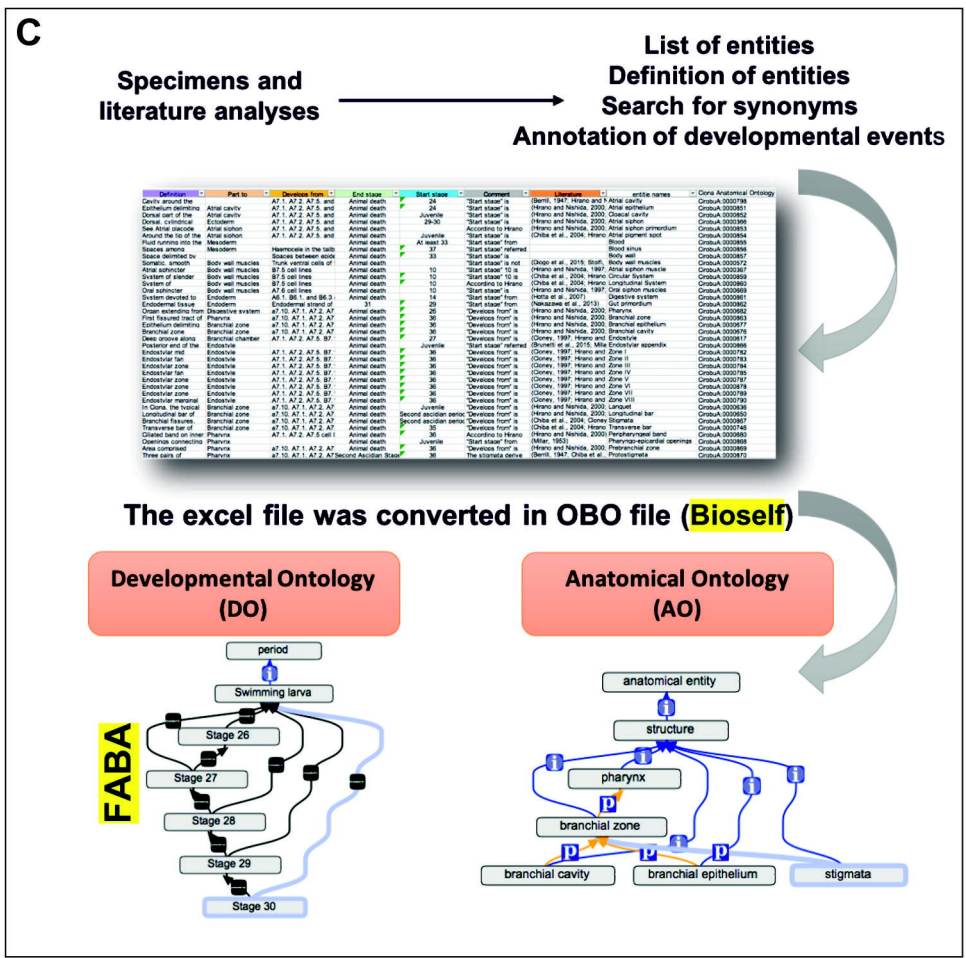

AO and DO incorporated with anatomical images

- Timelapse, Stereo Microscopy
- 3D/section images by CLSM
- Histological section images

TUNICANATO

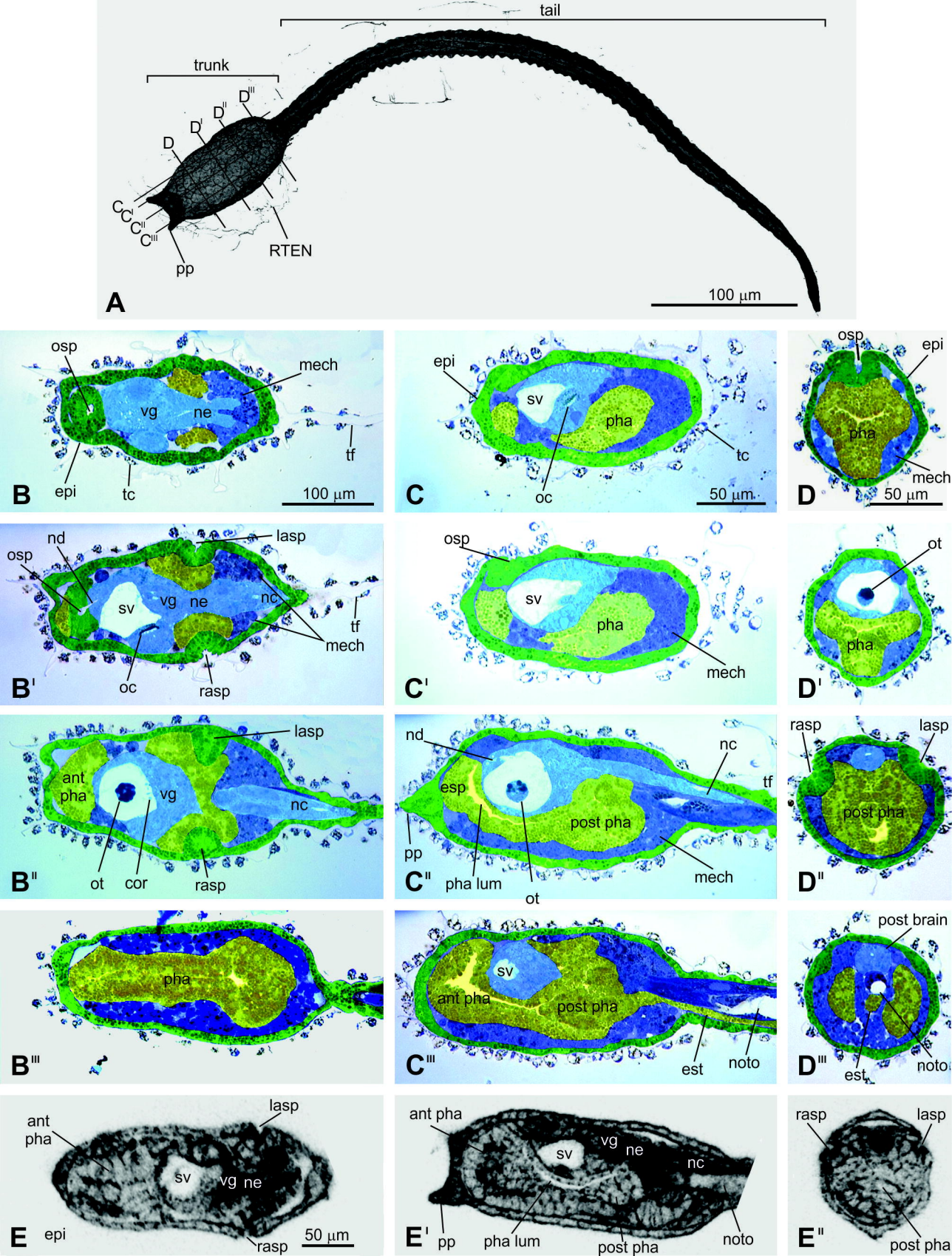
tail
trunk
D
D'
D''
D'''
C
C'
C''
C'''
RTEN
pp
A
100 µm
osp
mech
vg
ne
tf
epi
tc
B
100 µm
epi
sv
pha
tc
oc
C
50 µm
osp
epi
pha
mech
D
50 µm
nd
lasp
osp
sv
vg
ne
nc
tf
mech
oc
rasp
B'
osp
sv
pha
mech
C'
ot
pha
D'
ant
pha
vg
nc
lasp
ot
cor
rasp
B''
nd
nc
esp
tf
post pha
pp
pha lum
ot
mech
C''
rasp
lasp
post pha
D''
pha
B'''
sv
ant pha
post pha
est
noto
C'''
post brain
est
noto
D'''
ant
pha
lasp
sv
vg
ne
epi
rasp
50 µm
E
ant pha
vg
ne
sv
nc
pp
pha lum
post pha
noto
E'
rasp
lasp
post pha
E''

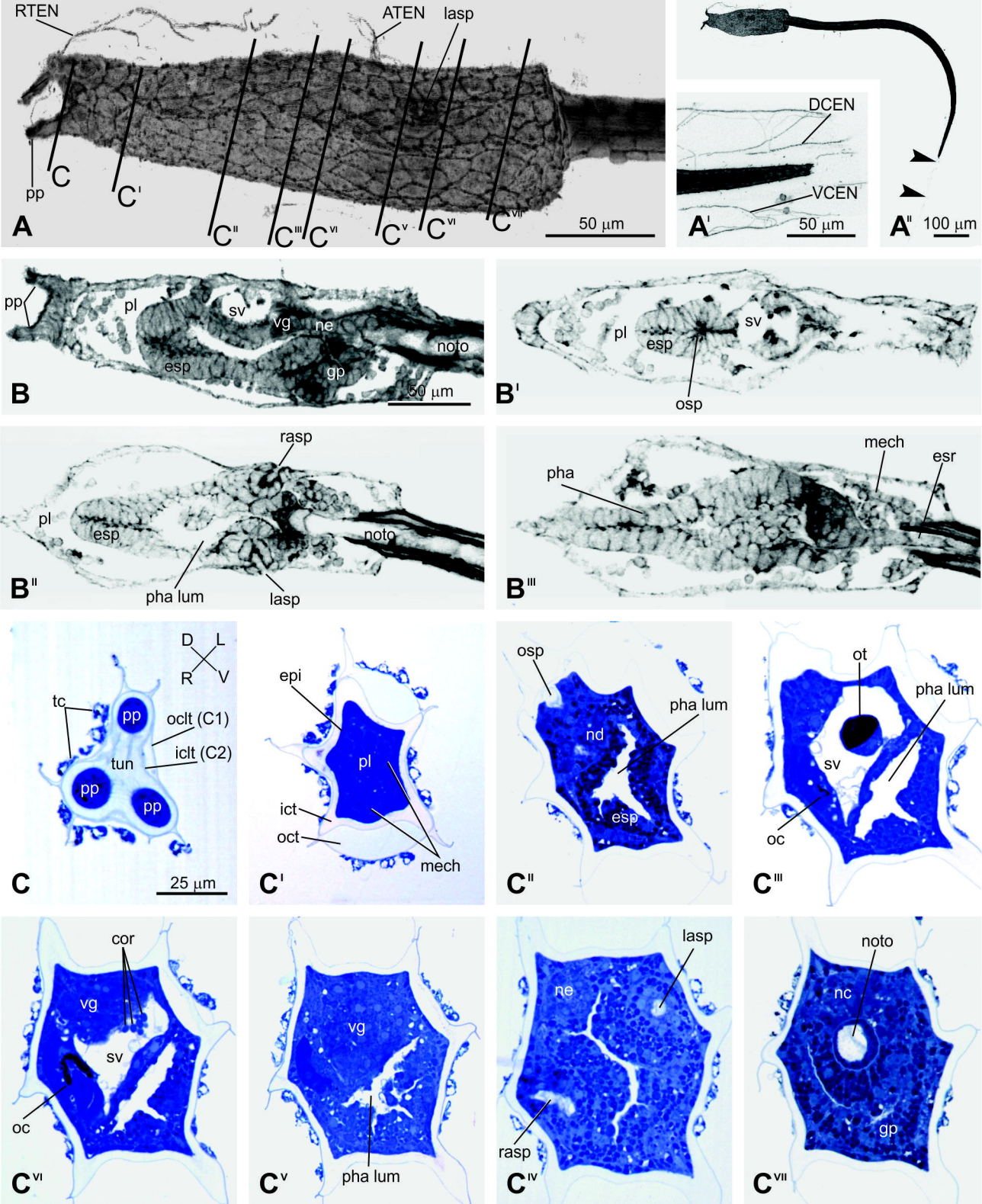
RTEN
ATEN
lasp
pp
C
C'
C''
C'''
C''''
C'''''
C''''''
C'''''''
A
50 µm
DCEN
VCEN
A'
50 µm
A''
100 µm
pp
pl
sv
vg
ne
noto
esp
gp
B
50 µm
pl
sv
esp
osp
B'
rasp
pl
esp
noto
pha lum
lasp
B''
pha
mech
esr
B'''
D
L
R
V
tc
pp
oclt (C1)
iclt (C2)
tun
pp
pp
C
25 µm
epi
pl
ict
oct
mech
C'
osp
pha lum
nd
esp
C''
ot
pha lum
sv
oc
C'''
cor
vg
sv
oc
C''''''
vg
pha lum
C'''''
lasp
ne
rasp
C''''
noto
nc
gp
C'''''''

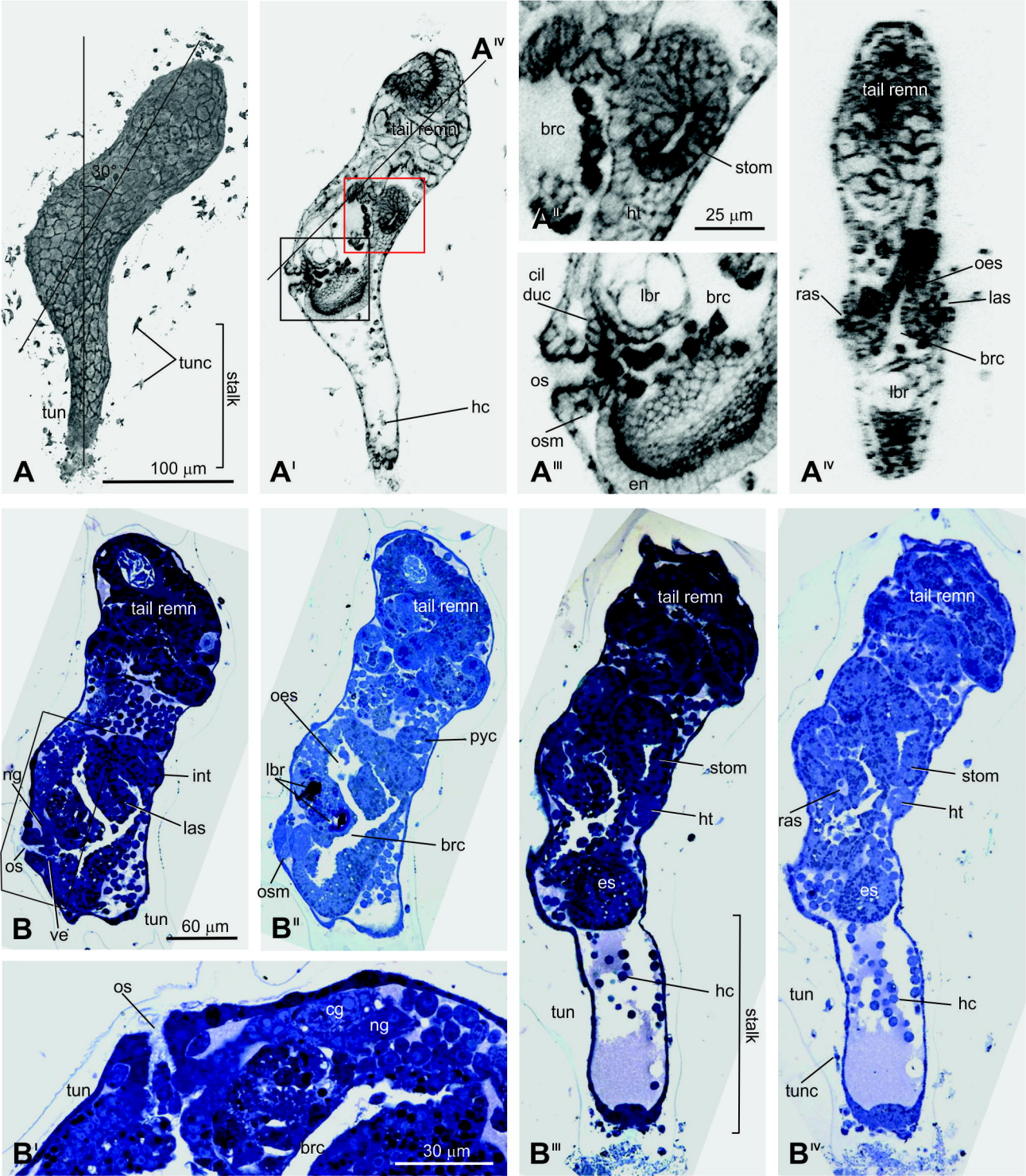
A
30°
tunc
stalk
tun
100 µm
A'
A^IV
tail remn
hc
A''
brc
stom
ht
25 µm
A'''
cil
duc
lbr
brc
os
osm
en
A^IV
tail remn
oes
ras
las
brc
lbr
B
tail remn
ng
int
las
os
ve
tun
60 µm
B''
tail remn
oes
pyc
lbr
brc
osm
B'
os
cg
ng
tun
brc
30 µm
B'''
tail remn
stom
ht
es
hc
tun
stalk
B^IV
tail remn
stom
ras
ht
es
tun
hc
tunc

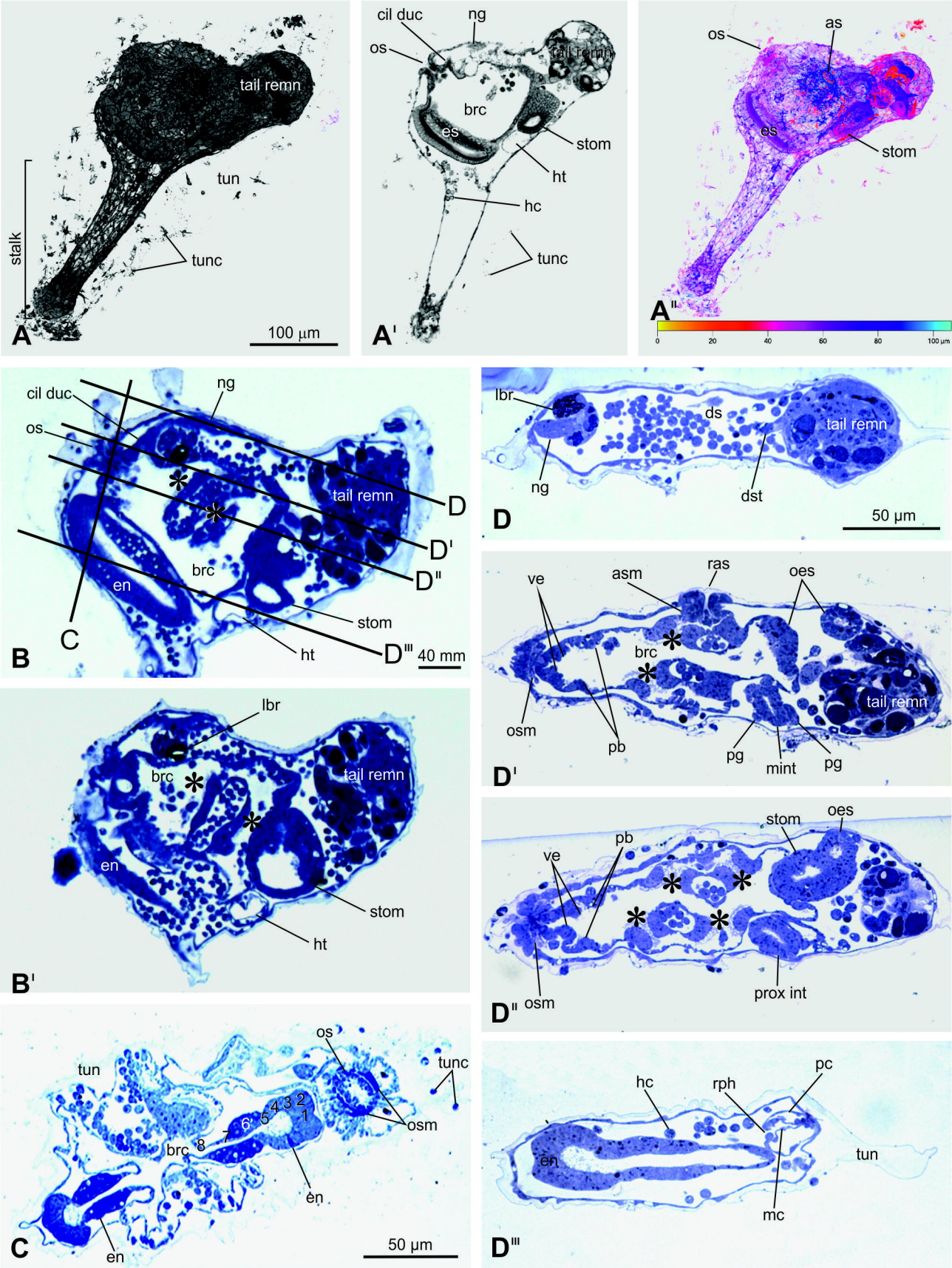
A
tail remn
tun
stalk
tunc
100 µm
A'
cil duc
ng
os
tail remn
brc
es
stom
ht
hc
tunc
A''
os
as
es
stom
0
20
40
60
80
100 µm
B
cil duc
ng
os
tail remn
D
D'
D''
brc
en
stom
C
ht
D'''
40 mm
B'
lbr
brc
tail remn
en
stom
ht
C
os
tun
tunc
osm
brc
en
en
50 µm
D
lbr
ds
tail remn
ng
dst
50 µm
D'
ve
asm
ras
oes
brc
tail remn
osm
pb
pg
mint
pg
D''
stom
oes
pb
ve
osm
prox int
D'''
hc
rph
pc
en
tun
mc

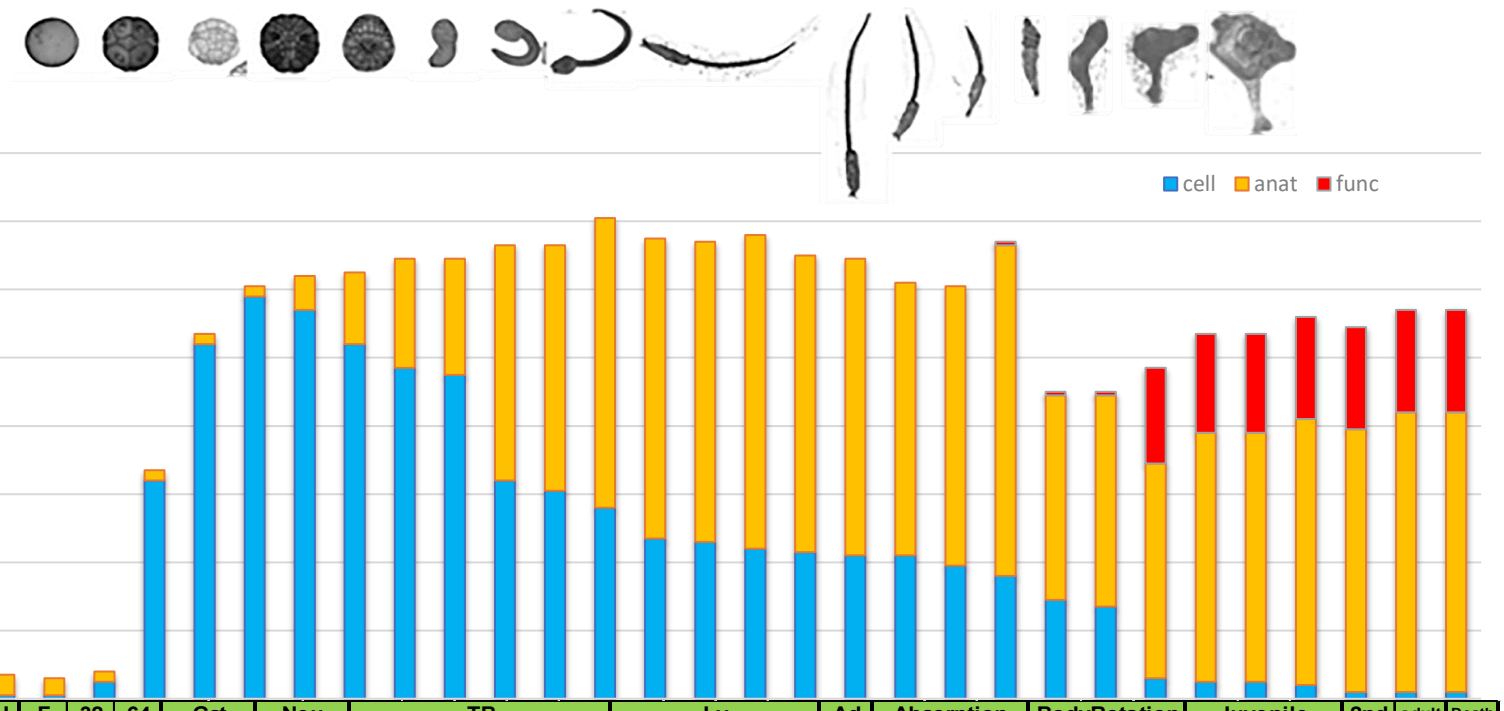

	U	F	32	64	Gst		Neu		TB					Lv				Ad	Absorption			BodyRotation			Juvenile			2nd	adult	Death
stage	0	1	6	8	10	12	14	16	17	18	22	24	25	26	27	28	29	30	31	32	33	34	35	36	37	38	Jv	2ndAs	adult	DEATH
cell	1	1	5	64	104	118	114	104	97	95	64	61	56	47	46	44	43	42	42	39	36	29	27	6	5	5	4	2	2	2
anato	6	5	3	3	3	3	10	21	32	34	69	72	85	88	88	92	87	87	80	82	97	60	62	63	73	73	78	77	82	82
func	0	0	0	0	0	0	0	0	0	0	0	0	0	0	0	0	0	0	0	0	1	1	1	28	29	29	30	30	30	30